https://doi.org/10.1093/plphys/kiad085 PLANT PHYSIOLOGY 2023: 192: 648–665

Plant Physiology®

Research Article

Tetratricopeptide repeat protein SlREC2 positively regulates cold tolerance in tomato

Ying Zhang [1,†] Yinxia Peng [1] Juan Liu [1] Jiarong Yan,[1] Kangyou Zhu [1] Xin Sun [4] Xin Bu [1] Xiujie Wang [1] Golam Jalal Ahammed [5,6] Yufeng Liu,[1] Zhouping Sun [1] Mingfang Qi [1] Feng Wang [1,2,3,*,†] and Tianlai Li [1,2,3,*]

1 College of Horticulture, Shenyang Agricultural University, Shenyang 110866, China
2 National & Local Joint Engineering Research Center of Northern Horticultural Facilities Design & Application Technology (Liaoning), Shenyang 110866, China
3 Key Laboratory of Protected Horticulture, Ministry of Education, Shenyang 110866, China
4 College of Land and Environment, Shenyang Agricultural University, Shenyang 110866, China
5 College of Horticulture and Plant Protection, Henan University of Science and Technology, Luoyang 471023, China
6 Henan International Joint Laboratory of Stress Resistance Regulation and Safe Production of Protected Vegetables, Henan University of Science and Technology, Luoyang 471023, China

*Author for correspondence: fengwang@syau.edu.cn (F.W.), tianlaili@126.com (T.L.)
The author responsible for distribution of materials integral to the findings presented in this article in accordance with the policy described in the Instructions for Authors (https://academic.oup.com/plphys/pages/General-Instructions) are: Feng Wang (fengwang@syau.edu.cn) and Tianlai Li (tianlaili@126.com).
†These authors contributed equally to this work.

Abstract

Cold stress is a key environmental constraint that dramatically affects the growth, productivity, and quality of tomato (*Solanum lycopersicum*); however, the underlying molecular mechanisms of cold tolerance remain poorly understood. In this study, we identified *REDUCED CHLOROPLAST COVERAGE* 2 (*SlREC2*) encoding a tetratricopeptide repeat protein that positively regulates tomato cold tolerance. Disruption of *SlREC2* largely reduced abscisic acid (ABA) levels, photoprotection, and the expression of C-REPEAT BINDING FACTOR (CBF)-pathway genes in tomato plants under cold stress. ABA deficiency in the *notabilis* (*not*) mutant, which carries a mutation in *9-CIS-EPOXYCAROTENOID DIOXYGENASE 1* (*SlNCED1*), strongly inhibited the cold tolerance of *SlREC2*-silenced plants and empty vector control plants and resulted in a similar phenotype. In addition, foliar application of ABA rescued the cold tolerance of *SlREC2*-silenced plants, which confirms that SlNCED1-mediated ABA accumulation is required for SlREC2-regulated cold tolerance. Strikingly, SlREC2 physically interacted with β-RING CAROTENE HYDROXYLASE 1b (SlBCH1b), a key regulatory enzyme in the xanthophyll cycle. Disruption of *SlBCH1b* severely impaired photoprotection, ABA accumulation, and CBF-pathway gene expression in tomato plants under cold stress. Taken together, this study reveals that SlREC2 interacts with SlBCH1b to enhance cold tolerance in tomato via integration of *SlNCED1*-mediated ABA accumulation, photoprotection, and the CBF-pathway, thus providing further genetic knowledge for breeding cold-resistant tomato varieties.

Introduction

Cold stress is one of the major environmental constraints on crop productivity, quality, and geographical distribution (Lesk et al. 2016). Tomato (*Solanum lycopersicum*) is widely grown in tropical, subtropical, and temperate regions, but tomato plants cannot survive long-term exposure to low temperatures. Thus, it is crucial to reveal the underlying mechanisms of cold responses in tomato for the molecular

Received October 19, 2022. Accepted January 18, 2023. Advance access publication February 10, 2023

breeding of cold-tolerant tomato varieties and expanding their distribution in high-latitude cold areas.

To withstand cold stress, immobile plants have evolved diverse regulatory systems that enable them to respond and adapt to adverse growth conditions. With decades of effort, a lot of key cold response-regulated factors and sophisticated mechanisms have been identified and revealed (Guo et al. 2018; Ding et al. 2020; Chen et al. 2021). During cold stress, the expression of many genes is induced by C-REPEAT BINDING FACTOR (CBF)/DEHYDRATION-RESPONSIVE ELEMENT BINDING FACTOR1 (DREB1) transcriptional activators (Thomashow 1999; Zhao et al. 2016). CBF/DREB1 proteins can directly associate with the promoters of *COLD-RESPONSIVE* (*COR*) genes and regulate their expression, thus enhancing plant cold tolerance (Stockinger et al. 1997; Song et al. 2021). INDUCER OF CBF EXPRESSION 1 (ICE1) also directly associates with the promoter of *CBFs* and activates *CBF* gene expression (Chinnusamy et al. 2003). The ICE1–CBF1–COR transcriptional cascade-regulated cold-signaling pathway has been extensively characterized (Shi et al. 2018). In addition, some classical phytohormones, such as abscisic acid (ABA), are also important for regulating cold stress responses. ABA-activated PYRBACTIN RESISTANCE-LIKE–TYPE 2C PROTEIN PHOSPHATASE–SUCROSE NONFERMENTING 1-RELATED PROTEIN KINASE2 (SnRK2)–ABA RESPONSIVE ELEMENT BINDING FACTOR pathway plays a critical role in ABA signal transduction and cold stress (Liu et al. 2018b; Gong et al. 2020; Wang et al. 2020a). Upon cold stress, cold-activated OPEN STOMATA 1 (OST1)/SnRK2.6 interacts with ICE1 and phosphorylates it, which disrupts the interaction of ICE1 and the E3 ligase HIGH EXPRESSION OF OSMOTICALLY RESPONSIVE GENE 1 and improves the protein stability of ICE1 (Ding et al. 2015; Lang and Zhu 2015). OST1 also enhances the transcriptional activity of ICE1 (Ding et al. 2015). Furthermore, OST1 phosphorylates the U-box E3 ligases PUB25 and PUB26, and enhances their activities for degradation of the transcription factor MYB15, which is a negative regulator of *CBFs* (Agarwal et al. 2006; Wang et al. 2019b). OST1 also stabilizes CBF proteins through phosphorylating BASIC TRANSCRIPTION FACTOR 3 under cold stress (Ding et al. 2018). Collectively, ABA promotes *CBF* gene expression and protein stability through these pathways to enhance plant cold tolerance. Moreover, OsbZIP73 interacts with OsbZIP71 to regulate cold tolerance through the ABA pathway in rice (*Oryza sativa*) (Liu et al. 2018a), which further demonstrates that ABA signaling plays a key role in the cold response.

During cold stress, the level of light incidence exceeds the utilization capacity of photosynthesis in plants, which can be harmful to the photosynthetic machinery and results in photoinhibition (Kingston-Smith et al. 1997). Plants dissipate excess light energy as thermal energy (nonphotochemical quenching, NPQ) to alleviate photodamage through the de-epoxidation state of the xanthophyll cycle (Takahashi and Badger 2011; Kromdijk et al. 2016). Furthermore, the turnover of D1 protein is critical for the photosystem II (PSII) repair process and NPQ induction during photoinhibition (Sundby et al. 1993). Interestingly, a study shows that REP27, a tetratricopeptide repeat (TRP) nuclear-encoded, plays a critical role in the D1 protein turnover and PSII repair from photodamage (Park et al. 2007). Therefore, it is of interest to investigate the roles of TPR motif-containing proteins in the regulation of cold-induced photoinhibition.

TPR proteins are involved in a variety of processes, such as peroxisomal import (Brocard and Hartig 2006), synaptic vesicle fusion (Young et al. 2003), and mitochondrial and chloroplastic import (Baker et al. 2007; Mirus et al. 2009). TPR domains highly degenerate at 34-amino acid repeats that are often present in tandem arrays, and are known to participate in the assembly of multiprotein complexes and protein–protein interactions (Lamb et al. 1995; Whitfield and Mainprize 2010). As reported, a variety of TPR proteins, such as PALE YELLOW GREEN 7, TRANSLOCATION OF CHLOROPLAST 64, LOW PSII ACCUMULATION 1, PLASTID TRANSCRIPTIONALLY ACTIVE CHROMOSOME PROTEINS 2, NAM ATAF1/2 CUC 2, and a nucleus-encoded tetratricopeptide-like repeat protein Mbb1, regulate protein transport and assembly, chloroplast development, mRNA processing and stability (Boudreau et al. 2000; Sohrt and Soll 2000; Vaistij et al. 2000; Peng et al. 2006; Pfalz et al. 2006; Stockel et al. 2006; Kalanon and McFadden 2008). Therefore, TPR motifs are important for both transcription and translation processes. However, little is known about the function and regulatory mechanism of TPR proteins in cold response.

In this study, we identified a tomato gene encoding a TPR protein, which is homologous to the REDUCED CHLOROPLAST COVERAGE (REC) proteins in Arabidopsis (*Arabidopsis thaliana*). Disruption of *SlREC2* largely reduced the cold tolerance and induced photoinhibition in tomato plants. Our analyses showed that *SlREC2* is essential for ABA accumulation and photoprotection in tomato plants during cold stress. Additionally, we demonstrate that the application of exogenous ABA can rescue the phenotype of *SlREC2*-silenced plants during cold stress, while the phenotypes of *SlREC2*-silenced plants are similar to that of nonsilenced plants in ABA-deficient *notabilis* (*not*) background, which carries a mutation in *9-CIS-EPOXYCAROTENOID DIOXYGENASE 1* (*SlNCED1*). Our results suggested that *SlREC2* acts upstream of *SlNCED1* to regulate ABA accumulation in tomato during cold stress. Strikingly, SlREC2 physically interacts with β-RING CAROTENE HYDROXYLASE 1b (SlBCH1b), a key regulatory enzyme in the carotenoid biosynthesis pathway. Disruption of *SlBCH1b* caused severe photoinhibition, reduced ABA accumulation, and CBF-pathway gene expression in tomato plants during cold stress. Together, our results suggest that SlREC2 interacts with SlBCH1b and acts synergistically to enhance cold tolerance in tomato by promoting ABA accumulation, CBF-pathway gene expression, and photoprotection. This study unravels a mechanism of SlREC2-regulated cold tolerance in tomato,

and provides further genetic knowledge for breeding cold-resistant tomato varieties.

Results

SlREC2 acts as a positive regulator in tomato cold tolerance

There are five *SlREC* homologs in tomato, and their deduced proteins contain conserved TPR domain with four TPR repeats, CLU central domain, and CLUstered mitochondria protein N-terminal domain (Supplemental Fig. S1). These five *SlREC* genes are clustered into four subgroups in *S. lycopersicum*, *A. thaliana*, *O. sativa*, *Mimulus lewisii*, and *Mimulus verbenaceus* (Fig. 1A). To investigate the physiological role of *SlRECs* in cold response in tomato plants, the transcription levels of *SlREC* genes were analyzed by reverse transcription quantitative PCR (RT-qPCR) (Fig. 1B). Notably, the transcript level of *SlREC2* dramatically upregulated in tomato plants after exposure to 4 °C for 6 h (Fig. 1B). To further understand the biological function of *SlREC2* in cold tolerance, we generated *SlREC2*-silenced plants (Supplemental Fig. S2A). The transcript level of *SlREC2* gene in the silenced lines was only 20% to 30% of that in empty vector plants, while transcript levels of other *SlREC* genes, such as *SlREC1-1*, *SlREC1-2*, *SlREC3*, and *SlFRIENDLY* in the *SlREC2*-silenced lines showed no obvious difference with those in empty vector plants (Supplemental Fig. S2B). Furthermore, there was no obvious difference in phenotypes between the *SlREC2*-silenced plants (pTRV-*SlREC2*) and control plants (pTRV) grown at 25 °C (Fig. 1C). However, compared with pTRV plants, leaves of pTRV-*SlREC2* plants showed severe wilting and necrosis after cold treatment (Fig. 1C), which was consistent with the results of histochemical staining with 3,3′-diaminobenzidine (DAB) and nitroblue tetrazolium (NBT) for in situ ROS accumulation (Fig. 1D). Consistently, the relative electrolyte leakage (REL), which is a representative indicator of cell membrane stability, was significantly higher in the *SlREC2*-silenced plants (pTRV-*SlREC2*) than that in control plants (pTRV) after cold treatment (Fig. 1E). Moreover, the value of net CO_2 assimilation rate (Pn) in pTRV-*SlREC2* plants grown at 4 °C was lower than that in pTRV plants (Fig. 1F). Chlorophyll fluorescence is used as a representative indicator of plant PSII performance under cold stress. No conspicuous difference in chlorophyll *a* fluorescence transient (OJIP) curves was observed between pTRV-*SlREC2* and pTRV plants before cold treatment. However, the OJIP curves of pTRV-*SlREC2* plants substantially decreased after cold stress compared with those in pTRV plants (Fig. 1G). In addition, PSII efficiency decreased significantly in pTRV-*SlREC2* compared with that in pTRV plants grown at 4 °C, but it was indistinguishable between pTRV-*SlREC2* and pTRV plants grown at 25 °C, as indicated by the maximum quantum yield of PSII (F_v/F_m), PI_{ABS}, and PI_{total} values (Fig. 1H; Supplemental Fig. S3). These results demonstrate that disruption of *SlREC2* enhances cold susceptibility in tomato. Furthermore, the expression of *SlCBF1* and *SlCBF2* increased in tomato plants after cold stress, but these genes exhibited significantly lower expression levels in *SlREC2*-silenced plants than those in pTRV plants (Supplemental Fig. S4). Taken together, these results suggest that *SlREC2* positively regulates cold tolerance in tomato.

SlREC2 acts as a positive regulator in alleviation of cold-induced photoinhibition

To analyze the role of *SlREC2* in cold-induced photoinhibition, we examined the F_v/F_m and the full oxidation of the P700 signal (P_m) in tomato plants. The results showed that there were no obvious differences in F_v/F_m and P_m between pTRV-*SlREC2* and pTRV plants grown at 25 °C (Fig. 2, A and B). However, cold stress decreased the levels of F_v/F_m and P_m more in pTRV-*SlREC2* plants than those in pTRV plants, which suggested that *SlREC2* played a positive role in the alleviation of cold-induced photoinhibition of PSII and PSI. To get a more detailed insight into the mechanisms of *SlREC2*-regulated alleviation of cold-induced photoinhibition, we measured a series of electron transport parameters of the photosystem. Cold stress caused a significant decrease in electron transport rate II (ETR(II)) and electron transport rate I (ETR(I)) in tomato plants, especially in *SlREC2*-silenced plants (Supplemental Fig. S5). In addition, the values of Y(II) dramatically downregulated in pTRV-*SlREC2* plants compared to those in pTRV plants grown at 4 °C (Fig. 2C). The decrease in Y(II) was related to the large decrease in photochemical quenching coefficient (qP) and quantum yield of regulated energy dissipation of PSII (NPQ) in *SlREC2*-silenced plants (Fig. 2C). As Y(II), Y(I) level was also lower in pTRV-*SlREC2* than pTRV plants when plants were exposed to cold conditions (Fig. 2D). It was possibly due to the obvious acceptor side limitation of PSI [Y(NA)], as evidenced by a higher level of Y(NA) in pTRV-*SlREC2* plants than those in pTRV plants (Fig. 2D). These results showed that disruption of *SlREC2* caused a drastic decrease in electron transport rate, photochemical energy conversion, and photoprotection after cold stress. Thus, *SlREC2* acts as a positive regulator in alleviating photoinhibition by improving energy dissipation of PSII, and reducing the acceptor-side limitations of PSI and the electron carrier overreduction in tomato plants during cold stress.

SlREC2-regulated cold tolerance in tomato is dependent on *SlNCED1*-mediated ABA accumulation

Since ABA plays an important role in cold response (Wang et al. 2016, 2019a), we aimed to investigate whether ABA is involved in the *SlREC2*-regulated cold tolerance in tomato. Results showed that there was no obvious difference in ABA accumulation between pTRV and pTRV-*SlREC2* plants grown at 25 °C, but ABA content was significantly lower in pTRV-*SlREC2* plants than that in pTRV plants when exposed to cold stress (Fig. 3A). Considering the change in ABA accumulation in *SlREC2*-silenced plants, we assumed that

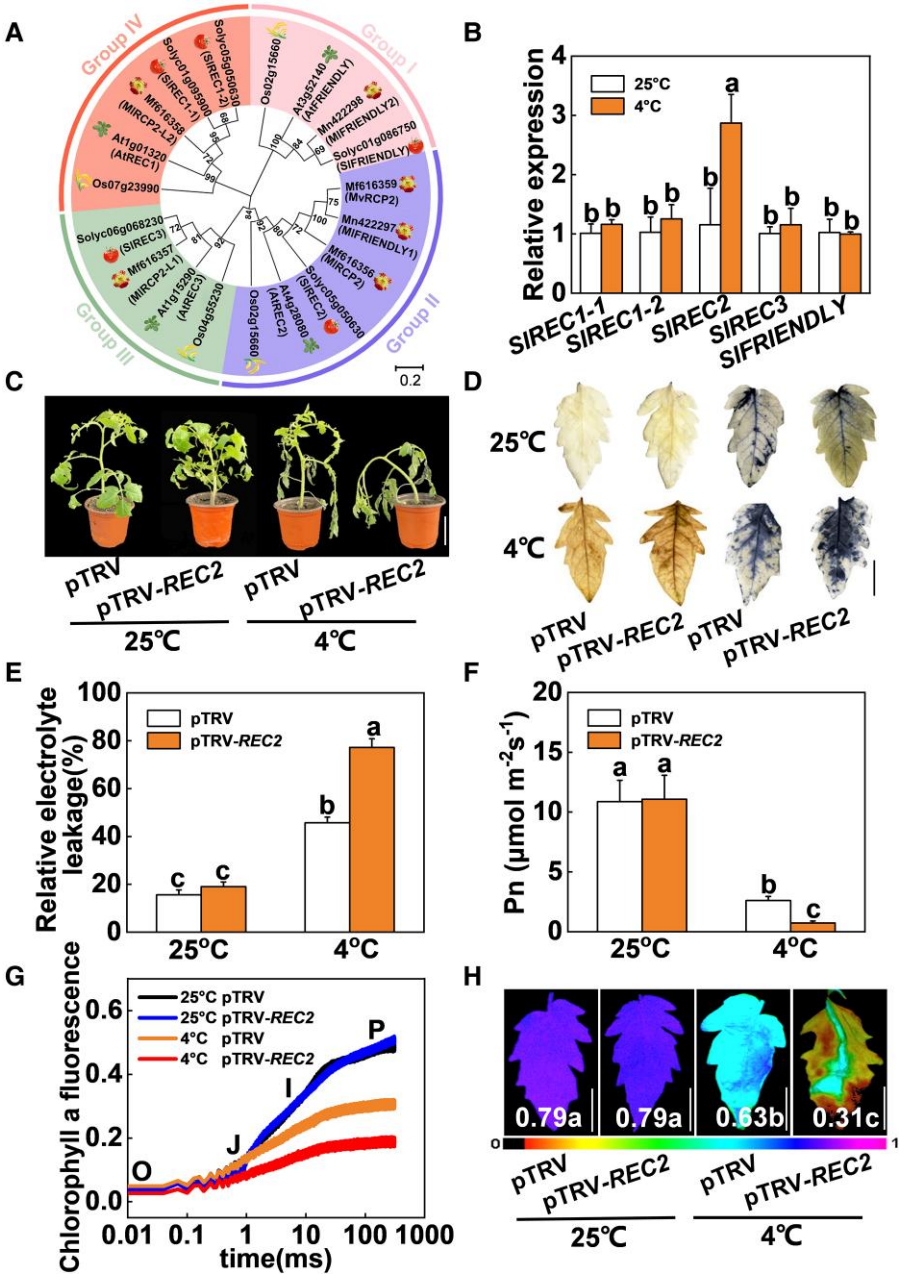

Figure 1. SlREC2 positively regulates cold tolerance in tomato. A) Phylogenetic analysis of REC proteins in *S. lycopersicum*, *A. thaliana*, *O. sativa*, *M. lewisii* and *M. verbenaceus*. The percentage at branch represents the posterior probabilities of amino acid sequences. B) Expression of *SlREC* family genes in tomato plants after exposure to 25 °C or 4 °C for 6 h. C, D) Phenotypes (C) and the accumulation of hydrogen peroxide (DAB staining) and superoxide (NBT staining) in tomato leaves (D) after the exposure of plants to 25 °C or 4 °C for 7 d. The plants (C) and leaves (D) were digitally extracted for comparison, respectively. Bar in (C), 5 cm. Bar in (D), 2 cm. E–H) REL (E), net CO_2 assimilation rate (Pn; F), the chlorophyll a fluorescence transient (OJIP) curves (G), and changes in the maximum photochemical efficiency of PSII (F_v/F_m) (H) in tomato wild-type (pTRV) and *SlREC2*-silenced plants (pTRV-*SlREC2*) after exposure to 25 °C or 4 °C for 7 d. The false-color code depicted at the bottom of the image ranges from 0 to 1.0, representing the level of damage in the leaves. Bars in (H), 2 cm. Data are presented as the means of three biological replicates (±SD). Different letters indicate significant differences ($P < 0.05$) according to Tukey's test.

SlREC2-regulated cold tolerance might be dependent on the ABA pathway. Therefore, the cold tolerance of pTRV and pTRV-*SlREC2* plants was examined after the application of ABA and ABA biosynthesis inhibitor nordihydroguaiaretic acid (NDGA). As shown in Supplemental Fig. S6A, the leaves of pTRV-*SlREC2* plant severely curled up compared to pTRV plants during cold stress, but with the application of exogenous ABA, the leaves of pTRV-*SlREC2* plants were similar to those in pTRV plants, as evidenced by the values of REL and F_v/F_m (Fig. 3, B–D), indicating that ABA largely

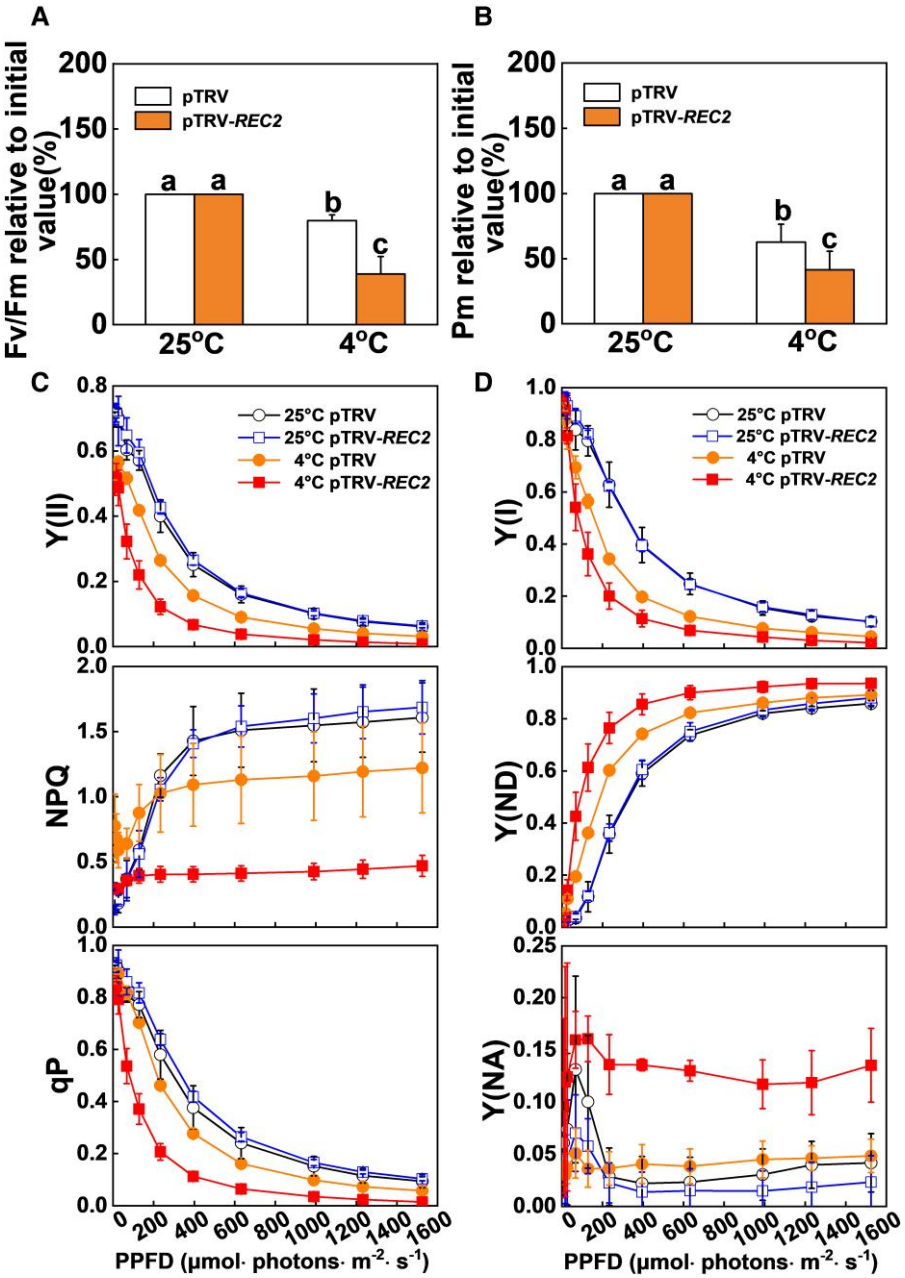

Figure 2. *SlREC2* is essential for alleviating cold-induced photoinhibition in tomato. A, C) Changes in PSII parameters, including the maximum photochemical efficiency of PSII (F_v/F_m; A), and the effective quantum yield of PSII [Y(II)], the quantum yield of regulated energy dissipation of PSII (NPQ), and the photochemical quenching coefficient (qP; C) in tomato wild-type (pTRV) and *SlREC2*-silenced plants (pTRV-*SlREC2*) after exposure to 25 °C or 4 °C for 5 d. B, D) Changes in PSI parameters, including the maximum P700 photooxidation level (P_m; B), and the quantum yield of PSI [Y(I)], the donor limitation of PSI [Y(ND)], the acceptor side limitation of PSI [Y(NA)] (D) in tomato wild-type (pTRV) and *SlREC2*-silenced plants (pTRV-*SlREC2*) after exposure to 25 °C or 4 °C for 5 d. Data are presented as the means of three biological replicates (±SD). Different letters indicate significant differences ($P < 0.05$) according to Tukey's test.

augmented the cold tolerance of pTRV-*SlREC2* plants. In addition, the application of exogenous NDGA enhanced the cold stress-induced leaf curling and wilting in both pTRV and pTRV-*SlREC2* plants, decreased F_v/F_m and increased REL (Fig. 3, B–D; Supplemental Fig. S6A). This finding suggests that *SlREC2*-regulated cold tolerance is dependent on the ABA pathway in tomato.

To protect PSII from photodamage, plants dissipate light energy as heat via activating NPQ (Muller et al. 2001; Wang et al. 2020b). Silencing of *SlREC2* in tomato plants impaired the cold-induced NPQ (Fig. 3E). Compared to the control, ABA treatment substantially induced NPQ in both pTRV and pTRV-*SlREC2* plants during cold stress, especially in pTRV plants, while NDGA impaired the NPQ induction by

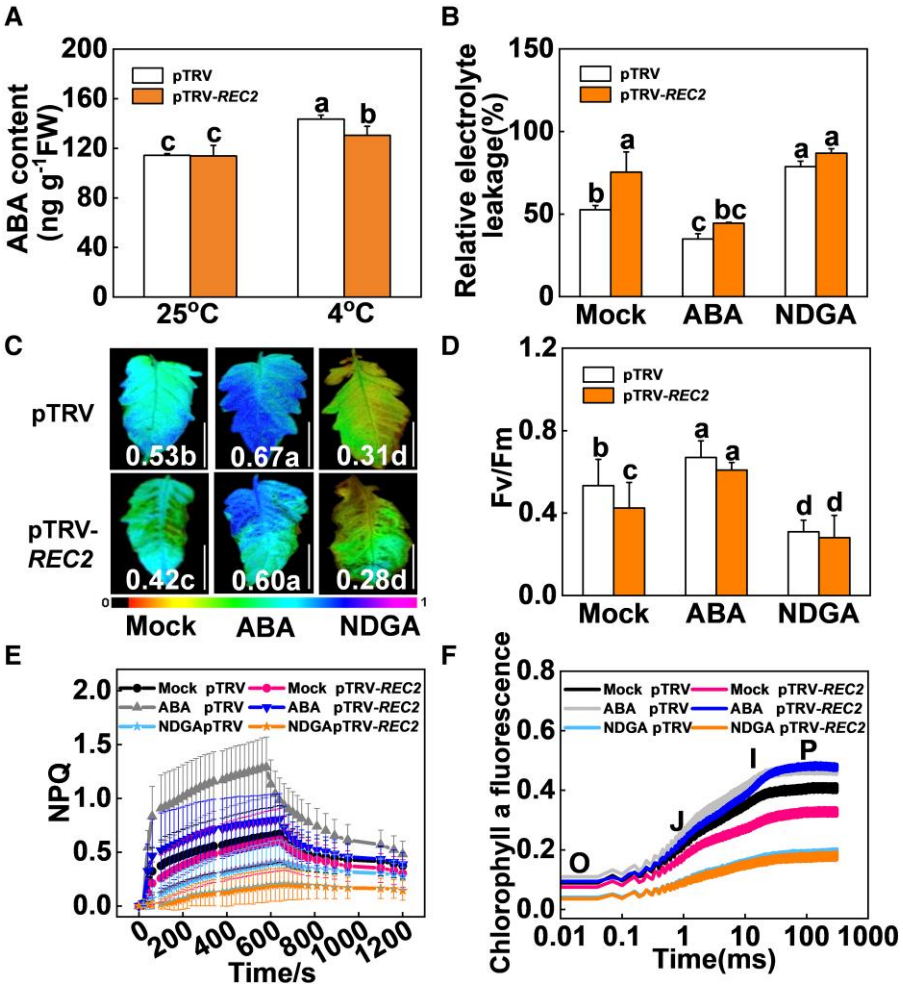

Figure 3. ABA plays a critical role in *SlREC2*-regulated cold tolerance in tomato. A), ABA content in tomato wild-type (pTRV) and *SlREC2*-silenced plants (pTRV-*SlREC2*) after exposure to 25 °C and 4 °C for 12 h. B–D) REL (B) and F_v/F_m (C, D) of pTRV and pTRV-*SlREC2* plants as influenced by foliar application of ABA and NDGA (ABA-inhibitor) under cold-stress conditions (4 °C for 7 d). The false-color code depicted at the bottom of the image ranges from 0 to 1.0, representing the level of damage in the leaves. Bars in (C), 2 cm. E, F) NPQ (E) and OJIP curves (F) of pTRV and pTRV-*SlREC2* plants as influenced by foliar application of ABA and NDGA under 4 °C for 5 d. Fifty micromolar ABA or NDGA was applied 12 h prior to exposure to cold conditions at 4 °C. Data are presented as the means of three biological replicates (±SD). Different letters indicate significant differences ($P < 0.05$) according to Tukey's test.

cold stress, which indicated that ABA enhanced the induction of NPQ during cold stress. We next measured the fast chlorophyll fluorescence kinetics (OJIP curve). The J-P rise was lower in pTRV-*SlREC2* plants than that in pTRV plants (Fig. 3F), indicating that disruption of *SlREC2* caused the over-reduction of plastoquinol (PQ) and quinone (Q_A). However, exogenous ABA treatment recovered the J-P rise of pTRV-*SlREC2* plants compared to pTRV plants (Fig. 3F). Furthermore, the exogenous application of ABA significantly increased the *SlCBF1* gene expression in the pTRV plants subjected to cold stress and completely rescued the *SlCBF1* gene expression of the pTRV-*SlREC2* plants (Supplemental Fig. S6B). Together, our results strongly suggest that *SlREC2* protects tomato plants from cold-induced photodamage through ABA-induced photoprotection and CBF pathways.

To investigate the mechanism of *SlREC2*-regulated ABA accumulation, the expression of some ABA biosynthetic genes was examined in pTRV and pTRV-*SlREC2* plants under cold stress. Interestingly, the expression of *SlNCED1*, a key gene in the ABA biosynthetic pathway, was significantly downregulated in the pTRV-*SlREC2* plants compared to that in the pTRV plants after cold stress (Fig. 4A). To further clarify the important role of *SlNCED1* in *SlREC2*-regulated cold tolerance, we disrupted the *SlREC2* gene in the wild-type and ABA-deficient mutant [*notabilis* (*not*)]. Results showed that the cold tolerance of pTRV in *not* background was much lower than that in the wild-type background, as indicated by an increased REL and a decreased F_v/F_m and *SlCBF1* gene expression (Fig. 4, B–D; Supplemental Fig. S7). However, the phenotypes, REL, F_v/F_m and *SlCBF1* gene expression of pTRV-*SlREC2* and pTRV in the *not* mutant background were similar (Fig. 4,

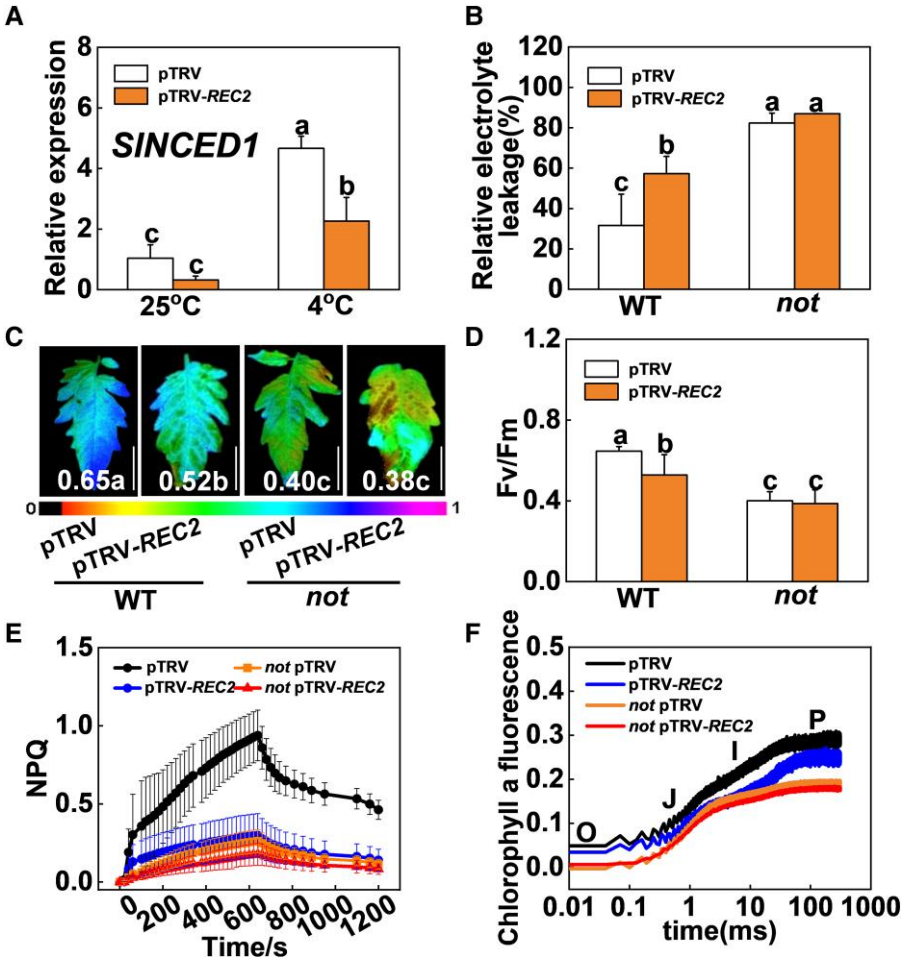

Figure 4. *SlNCED1* acts downstream of *SlREC2* in the cold response. A) *SlNCED1* gene expression in tomato wild-type (pTRV) and *SlREC2*-silenced plants (pTRV-*SlREC2*) after exposure to 25 °C and 4 °C for 6 h. B–D) REL (B) and F_v/F_m (C, D) in tomato plants when silenced or nonsilenced *SlREC2* (pTRV-*SlREC2* or pTRV) in wild type and *SlNCED1*-deficient mutant (*not*) after exposure to 4 °C for 7 d. The false-color code depicted at the bottom of the image ranges from 0 to 1.0, representing the level of damage in the leaves. Bars in (C), 2 cm. E, F) NPQ (E) and OJIP curves (F) in tomato plants when silenced or nonsilenced *SlREC2* (pTRV-*SlREC2* or pTRV) in wild-type and *SlNCED1*-deficient mutant (*not*) after exposure to 4 °C for 5 d. Data are presented as the means of three biological replicates (±SD). Different letters indicate significant differences ($P < 0.05$) according to Tukey's test.

B–D; Supplemental Fig. S7). In addition, the NPQ and the J-P rise in OJIP curves of pTRV plants in *not* background were similar to those *SlREC2*-silenced plants in *not* background (Fig. 4, E and F), which further indicated that *SlNCED1* acted downstream of *SlREC2* in response to cold stress. Taken together, our results suggest that *SlREC2*-regulated cold tolerance is dependent on *SlNCED1*-mediated ABA accumulation in tomato.

SlREC2 interacts with *SlBCH1b*

To further explore the regulatory mechanism of SlREC2 in cold response, we examined the subcellular localization of SlREC2 by transiently expressing *35S:SlREC2-GFP* in *Nicotiana benthamiana* leaf epidermal cells. SlREC2-GFP was intensively colocalized with the DAPI (4′, 6-diamidino-2-phenylindole) tagged nucleus marker throughout the cells (Fig. 5A). Consistently, a previous study showed that *REDUCED CAROTENOID PIGMENTATION1* (*RCP1*) in Monkeyflower, homologous to Arabidopsis REC proteins, localizes in the nucleus (Stanley et al. 2020). We performed a yeast two-hybrid (Y2H) screening and identified one of the SlREC2 interactors as SlBCH1b, a key regulatory enzyme in the carotenoid biosynthesis pathway (Fig. 5B). A bimolecular fluorescence complementation (BiFC) assay was performed in *N. benthamiana* to further verify the interaction between SlBCH1b and SlREC2 proteins. The reconstitution of yellow fluorescence protein (YFP) in the nuclei of epidermal cells was observed when co-infiltrated with SlREC2-nYFP and SlBCH1b-cYFP constructs, but was not observed in the negative controls (Fig. 5C). Furthermore, we corroborated the SlREC2–SlBCH1b interaction using firefly luciferase (LUC) complementation assays, where co-expression of SlREC2 with SlBCH1b in leaf cells of *N. benthamiana* generated strong luminescence signals that were not detected in the

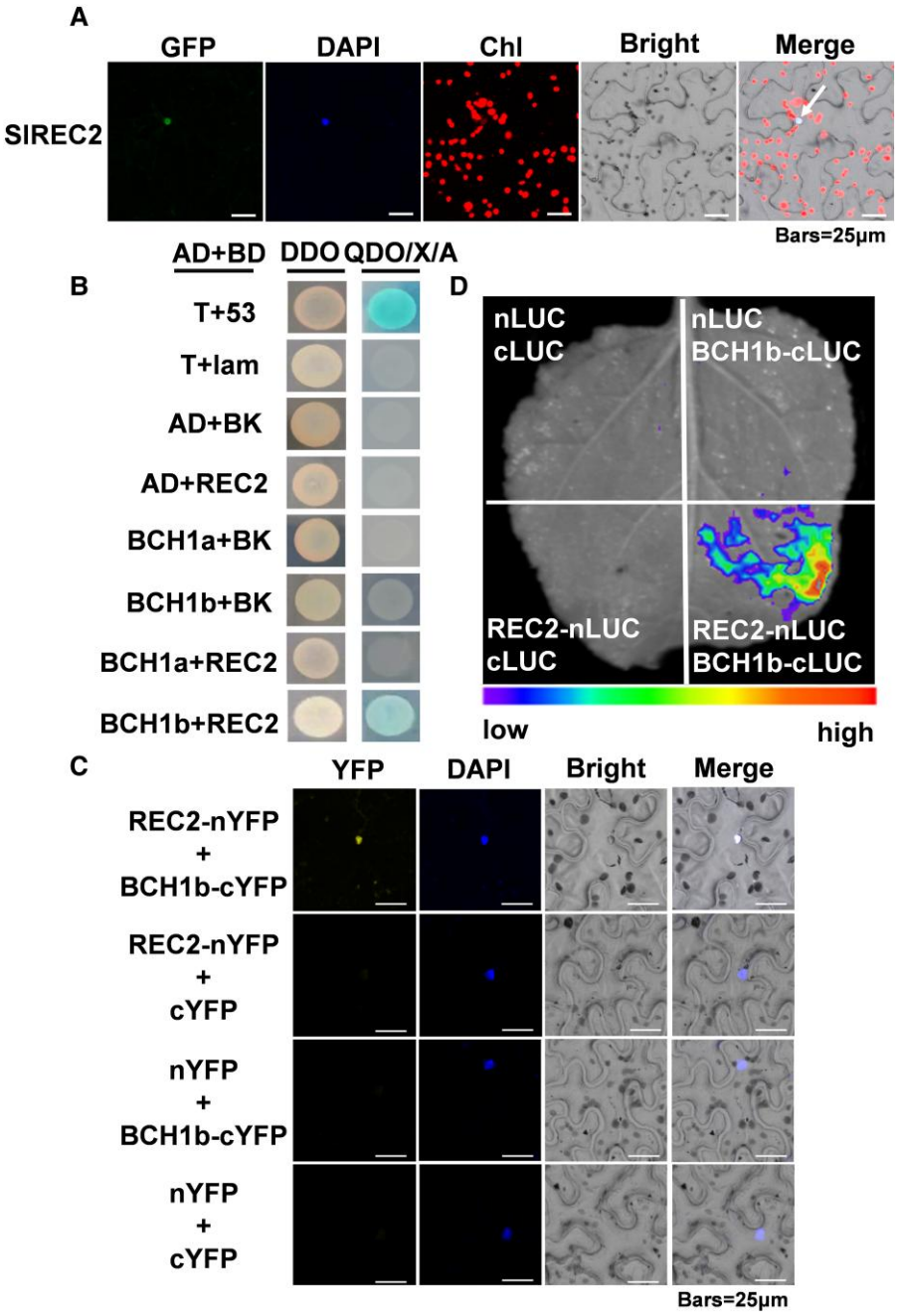

Figure 5. SlREC2 interacts with SlBCH1b. A) Subcellular localization of SlREC2 fused to GFP in *N. benthamiana* leaf mesophyll cells. GFP, green fluorescent protein; DAPI, a fluorescent dye (4′,6-diamidino-2-phenylindole) used to label normal nuclei; Chl, chlorophyll autofluorescence; Bright, brightfield. The arrowheads point to nuclei. Scale bars: 25 μm. B) Y2H assay showing the interaction of SlREC2 with SlBCH1b. SlREC2 was fused to the DNA activation domain (AD), while SlBCH1a and SlBCH1b were fused to the DNA binding domain (BD) of GAL4. DDO, yeast synthetic medium without Trp/Leu; QDO, yeast synthetic medium without Trp/Leu/His/Ade, but with 40 μg mL^{-1} of X-α-gal and 100 ng mL^{-1} aureobasidin A. C) Interaction of SlREC2 and SlBCH1b detected by BiFC analysis. SlBCH1b was fused to the C-terminal fragment of YFP (cYFP) and SlREC2 was fused to the N-terminal fragment of YFP (nYFP). The construct combinations were cotransformed into *N. benthamiana* leaves and expressed for 48 h. The signal was detected by confocal microscopy. Bar, 25 μm. D) LUC complementation imaging assay showing the interaction of SlREC2 and SlBCH1b in *N. benthamiana* leaves. SlREC2-nLUC/SlBCH1b-cLUC, SlREC2-nLUC/cLUC, nLUC/SlBCH1b-cLUC, and nLUC/cLUC were cotransformed into *N. benthamiana* leaves and investigated after 72 h. Similar results were obtained in three independent experiments.

control pairs (Fig. 5D). The above results indicate that SlREC2 interacts with the SlBCH1b protein.

SlBCH1b positively regulates cold tolerance in tomato plants

Subcellular localization assays indicated that SlBCH1b localized to the chloroplast and nucleus (Supplemental Fig. S8). Notably, cold stress induced the transcript level of *SlBCH1b* in tomato plants (Fig. 6A), but its transcript level was much lower in *SlREC2*-silenced plants (pTRV-*SlBCH1b*) than that in the control plants (pTRV) under cold stress (Fig. 6A), suggesting that *SlREC2* positively regulated *SlBCH1b* gene expression in tomato plants during cold stress. Next, we generated the *SlBCH1b*-silenced plants (pTRV-*SlBCH1b*) to further examine the role of *SlBCH1b* in the cold response (Supplemental Fig. S9A). pTRV-*SlBCH1b* plants exhibited an 85% reduction in the transcript levels of *SlBCH1b*, but no differences in *SlBCH1a* gene expression relative to those in pTRV plants (Supplemental Fig. S9B). Results showed that pTRV-*SlBCH1b* plants exhibited more severe wilting and necrosis during cold stress (Fig. 6, B and C), which suggested that *SlBCH1b* positively regulated cold tolerance in tomato plants. Furthermore, F_v/F_m and P_m displayed much lower in pTRV-*SlBCH1b* plants than those in pTRV plants under cold stress (Fig. 6, D–F). Moreover, the J-P rise in OJIP curves was lower in pTRV-*SlBCH1b* plants than that in pTRV plants during cold stress (Fig. 3F), indicating that disruption of *SlBCH1b* caused a decrease in PQ and Q_A in tomato plants. To get a detailed insight into *SlBCH1b* in the regulation of cold-induced photoinhibition, we investigated a number of PSII and PSI electron transport parameters. Impairment of the *SlBCH1b* gene in tomato plants caused a decrease in ETR(II) and ETR(I) during cold stress (Supplemental Fig. S10). In addition, some photosystem parameters, including Y(I), Y(NA), Y(ND), Y(II), qP, and NPQ, dramatically decreased in pTRV-*SlBCH1b* plants compared to pTRV plants during cold stress (Supplemental Fig. S10). The decrease in NPQ and qP might be the reason for the decrease in Y(II) in *SlBCH1b*-silenced plants during cold stress (Supplemental Fig. S10). Meanwhile, the obvious acceptor side limitation of PSI [Y(NA)] seemed to be the reason for the decrease in Y(I) in *SlBCH1b*-silenced plants (Supplemental Fig. S10). Consistently, compared with pTRV, disruption of *SlBCH1b* promoted the accumulation of hydrogen peroxide (H_2O_2) and superoxide ($O_2^{\bullet-}$) in the leaves of tomato plants during cold stress (Fig. 6H). Thus, these results suggest that disruption of *SlBCH1b* suppresses the capacity for photochemical energy conversion, electron transport rate, and photoprotection, leading to serious photoinhibition in tomato plants during cold stress.

To explore the molecular basis of *SlBCH1b* in the regulation of cold tolerance, we examined the transcript levels of cold marker genes *SlCBF1* and *SlCBF2* in pTRV and pTRV-*SlBCH1b* plants, and found that cold stress induced the expression of these genes in both tomato genotypes (Fig. 7, A and B). However, their transcription levels were much lower in pTRV-*SlBCH1b* plants than those in pTRV plants (Fig. 7, A and B), which indicated that *SlBCH1b* positively regulated CBF-pathway gene expression. In addition, *SlNCED1* gene expression and ABA accumulation were induced by low temperature, but they were obviously lower in pTRV-*SlBCH1b* plants than those in pTRV plants (Fig. 7, C and D). Furthermore, the transcript level of *ZEAXANTHIN EPOXIDASE 1* (*SlZEP1*), a critical xanthophyll cycle gene, and NPQ were induced in tomato plants after cold stress, but they were substantially decreased when *SlBCH1b* was disrupted in tomato plants (Fig. 7, E and F). Collectively, these results indicate that *SlBCH1b* enhances cold tolerance by activating the CBF pathway and inducing ABA accumulation and photoprotection.

SlREC2 and *SlBCH1b* work cooperatively to enhance cold tolerance in tomato

To investigate the genetic relevance of *SlREC2* and *SlBCH1b* in cold response, we generated the *SlREC2*-silenced plants, *SlBCH1b*-silenced plants, and their co-silenced plants (pTRV-*SlREC2*/*SlBCH1b*). After cold treatment, the cold tolerance of pTRV-*SlREC2* and pTRV-*SlBCH1b* decreased compared with pTRV, whereas their co-silenced plants showed more sensitivity to cold stress than only *SlREC2*- or *SlBCH1b*-silenced plants, as evidenced by a decrease in F_v/F_m and an increase in REL (Fig. 8, A–C; Supplemental Fig. S11). Consistently, compared to pTRV-*SlREC2* and pTRV-*SlBCH1b* plants, the pTRV-*SlREC2*/*SlBCH1b* plants displayed much more leaf necrosis, and increased accumulation of H_2O_2 and $O_2^{\bullet-}$ in the leaves after cold stress (Fig. 8, E and F), which indicated an additive role for *SlREC2* and *SlBCH1b* in regulating cold tolerance. Moreover, NPQ and the transcript levels of *SlCBF1* and *SlNCED1* were obviously lower in pTRV-*SlREC2*/*SlBCH1b* plants than those in pTRV-*SlREC2* or pTRV-*SlBCH1b* plants during cold stress (Fig. 8, D, G, and H). Therefore, these results demonstrate that *SlREC2* and *SlBCH1b* act synergistically to enhance cold tolerance in tomato.

Discussion

Tomato plants are sensitive to cold stress as they originated from tropical and subtropical regions. Investigating the mechanism of cold sensitivity in tomato is thus critical for the genetic improvement of this vegetable crop. Here, we identified a cold-induced gene *SlREC2*, encoding a TPR protein (Fig. 1, A and B). TPR proteins usually mediate protein–protein interactions or the assembly of multiprotein complexes (Cerveny et al. 2013). Previous studies show that TPR1 proteins in tomato and Arabidopsis interact with ethylene receptors, such as ETHYLENE RESPONSE1 (ETR1) and ETHYLENE RESPONSE SENSOR 1 (ERS1) (Lin et al. 2008, 2009). ETR1 and ERS1, members of HISTIDINE KINASES (HKs), have been reported to positively regulate

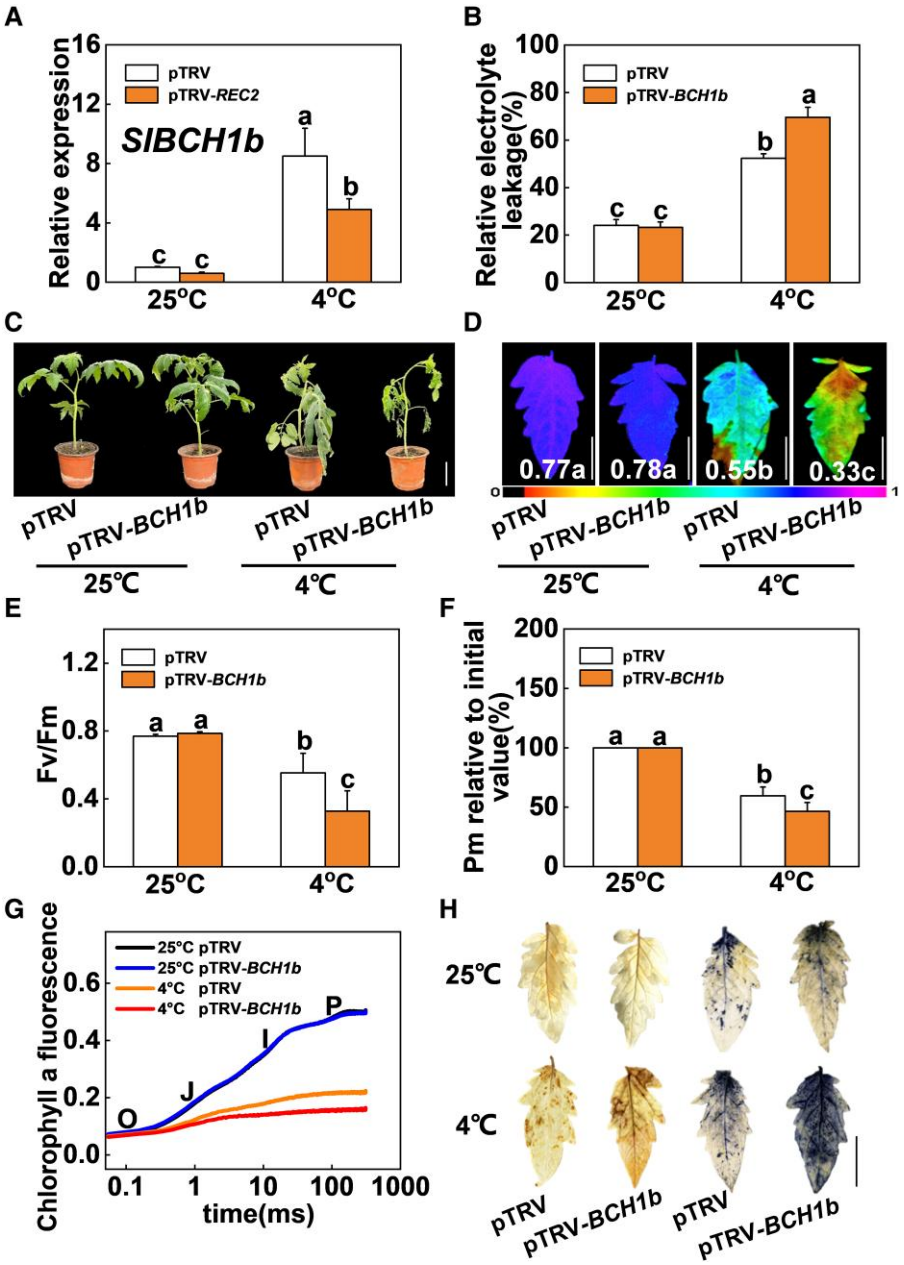

Figure 6. SlBCH1b positively regulates cold tolerance in tomato. A, B) *SlBCH1b* gene expression (A) and REL (B) in tomato wild-type (pTRV) and *SlBCH1b*-silenced plants (pTRV-*SlBCH1b*) after exposure to 25 °C or 4 °C for 6 h and 7 d, respectively. C–F) Phenotypes (C), F_v/F_m (D, E), and P_m (F) in pTRV and pTRV-*SlBCH1b* plants after exposure to 25 °C or 4 °C for 7 d. The plants were digitally extracted for comparison in (C). Bar in (C), 5 cm. Bars in (D), 2 cm. The false-color code depicted at the bottom of the image ranges from 0 to 1.0, representing the level of damage in the leaves. G, H) OJIP curves (G) and the accumulation of superoxide (NBT staining) and hydrogen peroxide (DAB staining) in tomato leaves (H) after pTRV and pTRV-*SlBCH1b* plants exposure to 25 °C or 4 °C for 7 d. The plants were digitally extracted for comparison. Bar in (H), 2 cm. Data are presented as the means of three biological replicates (±SD). Different letters indicate significant differences ($P < 0.05$) according to Tukey's test.

plant responses to freezing stress (Shi et al. 2012; Merchante et al. 2013), highlighting the importance of the HKs for cold signal perception in plants. The two transmembrane domains of HK Hik33 (intracellular HAMP and PAS domains), could sense changes in membrane rigidity via homodimerization and activation of the kinase, leading to the expression of cold-inducible genes (Murata and Los 2006; Shimura et al., 2012). Thus, as membrane-localized proteins, HKs can sense the changes in cell membrane fluidity during cold perception, interact with some TPR proteins, and modulate the expression of cold-inducible genes. Here, we found disruption of *SlREC2*-impaired cold tolerance in tomato (Fig. 1, C–F), which indicated that *SlREC2* positively regulates cold tolerance in tomato. However, how HKs sense the temperature

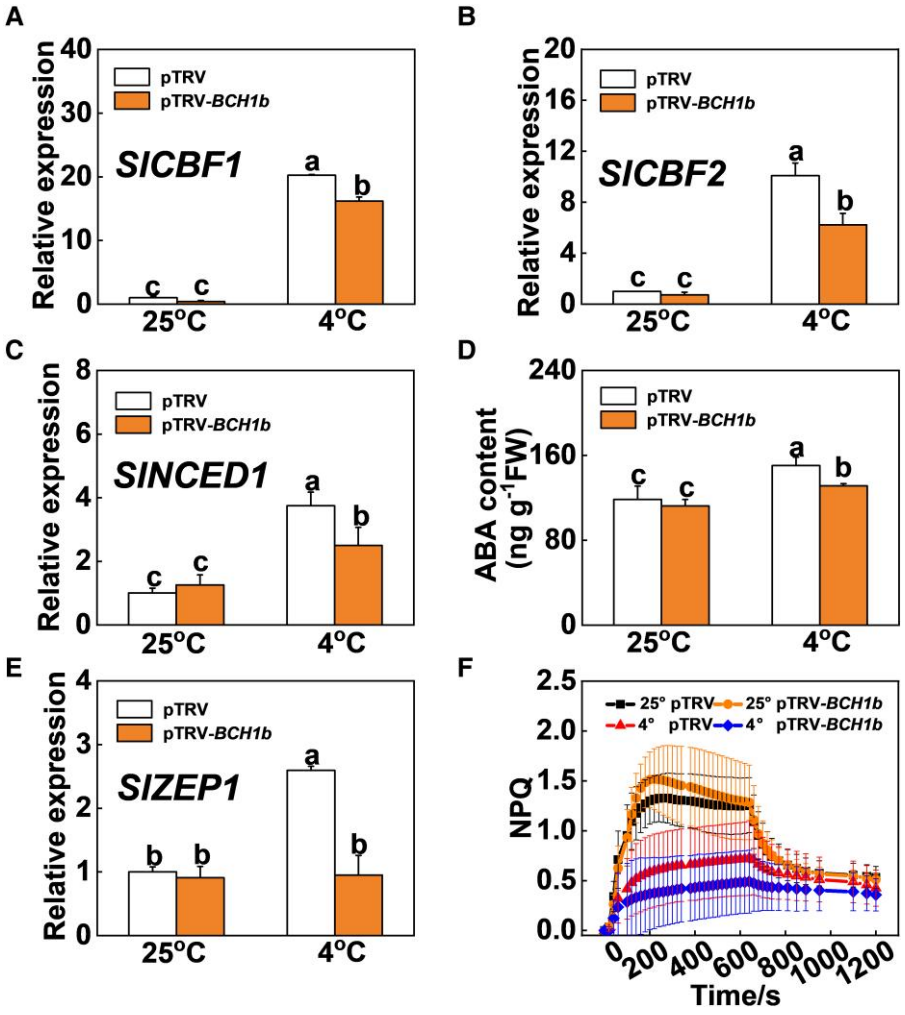

Figure 7. *SlBCH1b* regulates CBF-, ABA-, and xanthophyll cycle-pathway genes expression, ABA accumulation, and NPQ changes in response to cold stress. A, B) Expression of *SlCBF1* (A) and *SlCBF2* (B) genes in tomato wild-type (pTRV) and *SlBCH1b*-silenced plants (pTRV-*SlBCH1b*) after exposure to 25 °C and 4 °C for 6 h. C, D) Expression of *SlNCED1* (C) and accumulation of ABA (D) in pTRV and pTRV-*SlBCH1b* plants after exposure to 25 °C and 4 °C for 6 and 12 h, respectively. E, F) Changes of *SlZEP1* gene expression (E) and NPQ (F) in pTRV and pTRV-*SlBCH1b* plants after exposure to 25 °C and 4 °C for 6 h and 5 d, respectively. Data are presented as the means of three biological replicates (±SD). Different letters indicate significant differences ($P < 0.05$) according to Tukey's test.

signal and regulate *SlREC2* remains an exciting topic for future investigation.

Our results showed that disruption of *SlREC2* led to cold-induced photoinhibition in tomato, as evidenced by a decrease in F_v/F_m and P_m (Figs. 1H and 2, A and B). The capacity for electron transport rate, photoprotection, and photochemical energy conversion seriously decreased in *SlREC2*-silenced plants compared to the control plants under cold stress (Figs. 1G and 2, C and D; Supplemental Figs. S3 and S5). Compared to the control plants, NPQ and OJIP curve substantially deceased, whereas Y(NA) increased in the *SlREC2*-silenced plants, indicating that *SlREC2* alleviated cold-induced photoinhibition through dissipation of excess light energy as thermal energy, and reducing the limitations of PSI acceptor-side and over-reduction of electron carriers. Recent studies have shown that TPR proteins are involved in chloroplast gene expression and chlorophyll biosynthesis (Hu et al. 2014), thylakoid membrane biogenesis (Schottkowski et al. 2009), protein turnover (Park et al. 2007), photosystem assembly and repair (Park et al. 2007, Heinnickel et al. 2016). Arabidopsis REC1 is an extraplastidic protein that regulates the size of the chloroplast compartment (Larkin et al. 2016). CGL71 is a TPR protein that is involved in chloroplast thylakoid membrane formation, and protecting PSI from oxidative disruption during assembly in *Chlamydomonas reinhardtii* (Heinnickel et al. 2016). In addition, TPR motifs interact with PsaA and PsaD to contain the stability of PSI (Naver et al. 2001). Furthermore, REP27, a TRP protein in *C. reinhardtii*, enhances D1-reaction center protein turnover and PSII repair from photodamage (Park et al. 2007). Therefore, *SlREC2* may alleviate cold-induced photoinhibition by enhancing D1 protein turnover,

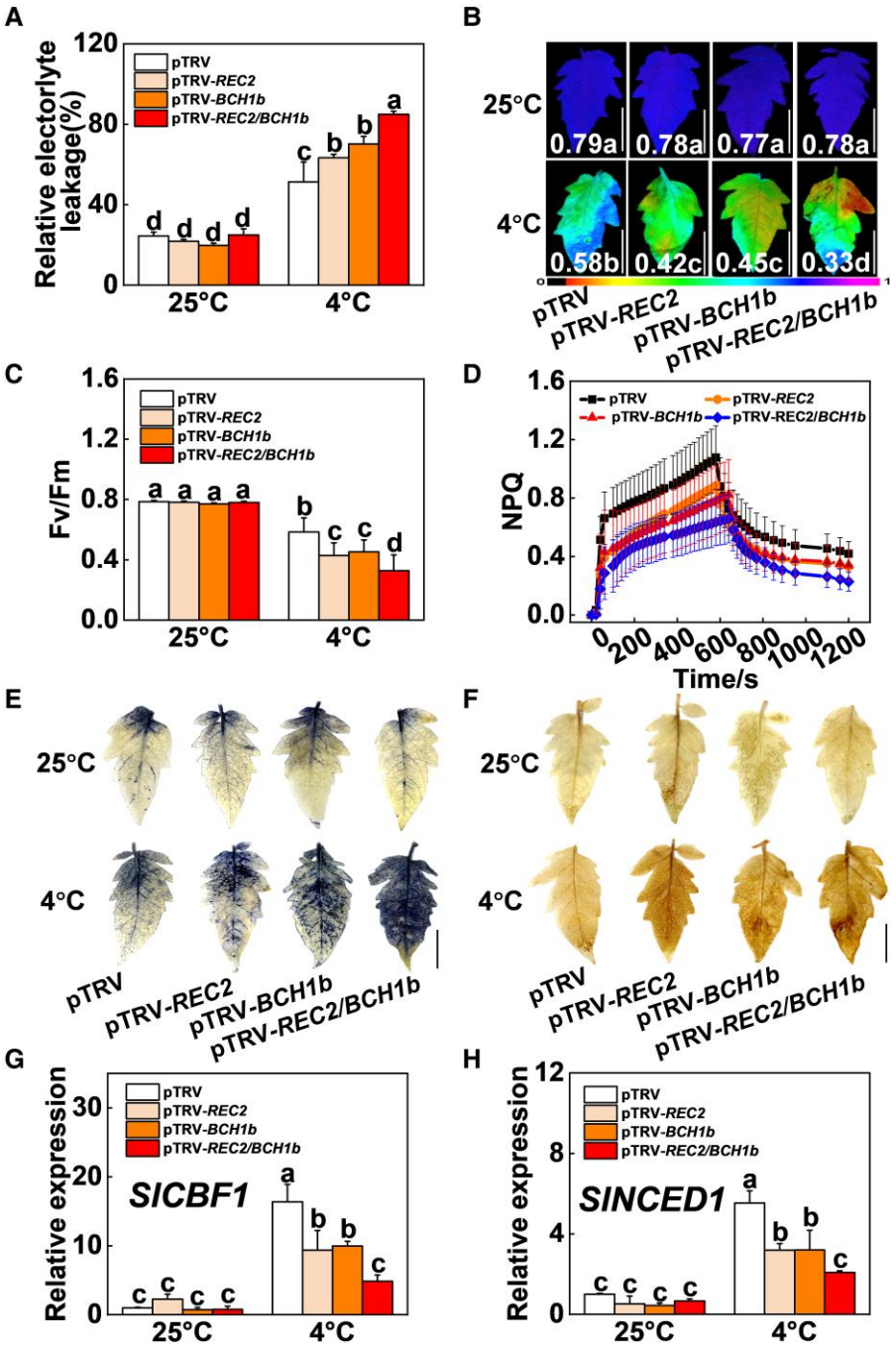

Figure 8. *SlREC2* and *SlBCH1b* act additively to enhance cold tolerance in tomato plants. A–F) REL (A), F_v/F_m (B, C), NPQ (D), the accumulation of superoxide (NBT staining; E) and hydrogen peroxide (DAB staining; F) in tomato wild-type (pTRV), *SlREC2*-silenced plants (pTRV-*SlREC2*), *SlBCH1b*-silenced plants (pTRV-*SlBCH1b*), and the co-silenced plants of these two genes (pTRV-*SlREC2*/*SlBCH1b*) after exposure to 25 °C or 4 °C for 7 d. Bars in (B), 2 cm. The false-color code depicted at the bottom of the image ranges from 0 to 1.0, representing the level of damage in the leaves. The plants were digitally extracted for comparison in (E) and (F), respectively. Bars in (E) and (F), 2 cm. G, H) Expression of *SlCBF1* and *SlNCED1* in pTRV, pTRV-*SlREC2*, pTRV-*SlBCH1b*, and pTRV-*SlREC2*/*SlBCH1b* plants after exposure to 25 °C or 4 °C for 6 h. Data are presented as the means of three biological replicates (±SD). Different letters indicate significant differences ($P < 0.05$) according to Tukey's test.

photosystem assembly and repair, and reducing the over-reduction of electron carriers in tomato plants.

Carotenoids function as critical pigments in light harvesting and components of the photosynthesis system for protecting the photosynthetic apparatus from photooxidative damage (Baroli and Niyogi 2000; Dall'Osto et al. 2007). In addition, carotenoids also act as precursors for ABA biosynthesis (Marin et al. 1996). *RCP1* and *RCP2*, which are

homologous to Arabidopsis REC proteins, regulate the carotenoid biosynthesis in *Mimulus* flowers (Sagawa et al. 2016; Stanley et al. 2020). It is worth noting that *RCP1* belongs to the R2R3-MYB family and has a function in ABA response (Park et al. 2011). Thus, we hypothesized that *SlREC2* may regulate cold tolerance through the ABA pathway in tomato. Consistent with our hypothesis, we observed that disruption of *SlREC2* impaired the ABA accumulation in tomato plants during cold stress (Fig. 3A). Interestingly, the phenotype and photosynthetic capacity were rescued in *SlREC2*-silenced plants after the application of exogenous ABA during cold stress (Fig. 3, B–F; Supplemental Fig. S6), which indicated that ABA plays an important role in *SlREC2*-regulated cold tolerance and photoprotection in tomato. In agreement with this, we previously demonstrated that ABA signaling enhances photoprotection in tomato during cold stress (Wang et al. 2018). In addition, the TETRATRICOPEPTIDE-REPEAT THIOREDOXIN-LIKE 1, a TPR-containing protein, has been found to function in the regulation of ABA signaling and abiotic stress responses (Rosado et al. 2006). Interestingly, disruption of *SlREC2* inhibited the cold-induced *SlNCED1* expression in tomato plants during cold stress (Fig. 4A), which indicated that *SlNCED1* might be a key regulator in *SlREC2*-regulated ABA accumulation in tomato. To confirm this, we disrupted the *SlREC2* in *not* mutant and its wild type. Results showed that there were no obvious differences between *SlREC2*-silenced plants and the control plants (pTRV) in the *not* mutant background during cold stress (Fig. 4, B–F; Supplemental Fig. S7), suggesting that *SlNCED1*-mediated ABA accumulation acts downstream of *SlREC2* in regulating cold tolerance in tomato.

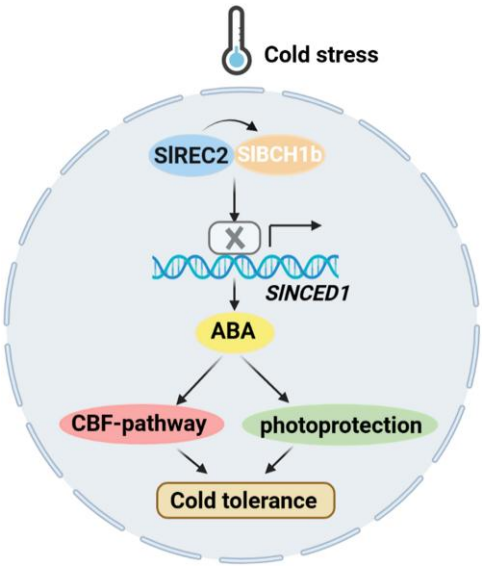

Figure 9. A proposed model explaining the regulatory mechanism of *SlREC2*-mediated cold response in tomato. *SlREC2* transcript levels significantly upregulated when tomato plants are exposed to cold stress. SlREC2 rapidly induces the gene expression of *SlBCH1b* and interacts with SlBCH1b protein during cold stress. Subsequently, SlREC2 and SlBCH1b act synergistically to induce *SlNECD1*-mediated ABA accumulation most likely through enhancing their protein stability or the transcriptional activity of other unknown transcription factors (X) on the *SlNECD1* gene. ABA increases the expression levels of *CBF* genes and photoprotection, thereby enhancing cold tolerance in tomato.

In this study, we found that SlREC2 interacted with SlBCH1b (Fig. 5, B–D). BCH, a carotene hydroxylase, catalyzes β-ionone ring hydroxylation toward β, β-xanthophylls in zeaxanthin biosynthesis (Kim et al. 2009; Walter and Strack 2011), which plays a critical role in xanthophyll cycle (Jahns et al. 2009). It was reported that overexpression of the tomato *CrtR-b2* (carotene beta hydroxylase) gene increased xanthophyll contents (D'Ambrosio et al. 2011). To enhance the xanthophyll content and alleviate cold-induced photoinhibition, the transcript level of *SlBCH1b* in tomato plants was upregulated during cold stress (Fig. 6A). In the xanthophyll cycle, ZEP catalyzes zeaxanthin (Z) to antheraxanthin (A), which produces violaxanthin (V), while V can be reconverted to Z under violaxanthin de-epoxidase catalysis. Z is essential for the thermal dissipation of excess energy (Niyogi et al. 1998). qE-dependent NPQ is regulated by the de-epoxidation state of the xanthophyll cycle pigments (Kromdijk et al. 2016). Here, we found that *SlZEP1* gene expression, NPQ and photochemical energy conversion were lower in *SlBCH1b*-silenced plants than those in the control plants (pTRV) during cold stress (Figs. 6, D–G and 7, E and F; Supplemental Fig. S10), indicating that *SlBCH1b* alleviates cold-induced photoinhibition through xanthophyll cycle and thermal dissipation in tomato.

It is well known that NCED can catalyze V and neoxanthin to produce ABA (Bouvier et al. 1998). Our results showed that *SlNCED1* gene expression and ABA accumulation were significantly lower in *SlBCH1b*-silenced plants than those in the control plants during cold stress (Fig. 7, C and D), especially in the *SlREC2* and *SlBCH1b* co-silenced plants (Fig. 8H). These results indicate that *SlREC2* and *SlBCH1b* act synergistically to confer *SlNCED1*-mediated ABA accumulation at least in the process of cold tolerance. Given the synergistic interactions between SlREC2 and SlBCH1b, the SlREC2 protein most likely has regulatory targets nonoverlapping with SlBCH1b in the control of *SlNCED1*-mediated ABA accumulation, although SlREC2 target genes are elusive so far. Besides the SlBCH1b-dependent pathway, SlREC2 alone can also regulate *SlNCED1* gene expression through other pathways. Moreover, other components might be involved in regulating SlBCH1b. Probably, each individual member deals with mild ABA responses, but the physical interaction between SlREC2 and SlBCH1b facilitates strong and robust ABA responses by enhancing their protein stability or the transcriptional activity of other transcription factors (X) to regulate the *SlNCED1* gene expression (Fig. 9). Similarly, OsTPR075 interacts with FT-INTERACTING PROTEIN1 (OsFTIP1) and OsFTIP9, and enhances their ability to transport florigen (Zhang et al. 2022). Notably, the *SlREC2* and *SlBCH1b* co-silenced plants exhibited higher susceptibility to cold stress than *SlREC2*- or *SlBCH1b*-silenced plants

(Fig. 8, A–F; Supplemental Fig. S11C), which was also supported by the expression of *SlCBF1* gene. Cold induction of the *SlCBF1* gene was compromised in *SlREC2*- and *SlBCH1b*-silenced plants and more profoundly in the co-silenced plants (Fig. 8G). In agreement with the findings of ABA-promoted *CBF* gene expression and protein stability (Agarwal et al. 2006; Ding et al. 2015; 2018; Wang et al. 2019b), our results suggest that SlREC2 and SlBCH1b act additively to confer ABA accumulation, resulting in increased expression levels of *CBF*s and enhanced photoprotection, and thereby conferring cold tolerance to tomato plants (Fig. 9). This study provides valuable information for potential genetic modification and breeding of tomato in response to cold stress.

Materials and methods

Plant materials and growth conditions

Seeds of the ABA biosynthesis mutant (*not*) in the tomato (*S. lycopersicum*) cv Ailsa Craig background were purchased from the Tomato Genetics Resource Center (http://tgrc.ucdavis.edu). As done previously, we used the virus-induced gene silencing (VIGS) technique with tobacco rattle virus (TRV)-based vectors (pTRV1/2) to silence the *SlREC2* and *SlBCH1b* genes (Wang et al. 2016; Bu et al. 2021). The VIGS vectors of *SlREC2* and *SlBCH1b* genes were constructed with the gene-specific primers as listed in Supplemental Table S1. VIGS was carried out as described previously (Wang et al. 2016; Bu et al. 2021). The VIGS plants were grown at 22 °C/20 °C (day/night) under 12-h light/dark cycles (a photosynthetic photon flux density of 400 μmol m^{-2} s^{-1}). The silencing efficiency of the targeted genes was examined by RT-qPCR.

Cold tolerance assays and cold stress treatment

We used REL and chlorophyll fluorescence to analyze the cold tolerance of tomato plants. The REL was examined in tomato plants after cold treatment at 4 °C for 7 d, as described previously (Wang et al. 2022). The P700 redox state measurement and chlorophyll fluorescence were investigated with Dual-PAM-100 (Heinz Walz, Effeltrich, Germany) as previously described (Wang et al. 2020b; Bu et al. 2021). Plants were kept in dark conditions for 30 min before the measurements. The effective quantum yield of PSII [Y(II)] and PSI [Y(I)], photochemical quenching coefficient (qP), quantum yield of regulated energy dissipation of PSII (NPQ), P700 maximum photooxidation level (P_m), acceptor-side and donor-side limitation of PSI [Y(NA) and Y(ND)], and the electron transport rate (ETRI or ETRII) were investigated (Wang et al. 2020b; Bu et al. 2021). The NPQ curves and maximum quantum yield of PSII (F_v/F_m) were measured by the Imaging-PAM (IMAG-MAXI; Heinz Walz, Effeltrich, Germany) (Wang et al. 2018). In addition, we analyzed the polyphasic chlorophyll *a* fluorescence transients (OJIP) curves with the JIP-test method (Kalaji et al. 2014; Wang et al. 2020b).

For cold-stress treatments, tomato seedings at the six-leaf stage were treated for a temperature of 25 °C or 4 °C in controlled-environment growth chambers (Ningbo Jiangnan Instrument Factory, Ningbo, China) for 7 d, unless otherwise stated.

Gas exchange and histochemical staining

The net CO_2-assimilation rate (Pn) was measured on the third leaf from the bottom of each plant with an infrared gas analyzer-based portable photosynthesis system (LI-6400; LI-COR, Inc., Lincoln, NE, USA). The measured conditions were a leaf temperature of 25 °C, a relative air humidity of 85%, a CO_2 concentration of 400 μmol mol^{-1}, and a photosynthetic photon flux density of 630 μmol m^{-2} s^{-1}.

Histochemical staining of hydrogen peroxide (H_2O_2) and superoxide ($O_2^{\bullet-}$) was conducted in tomato leaves with DAB and NBT, respectively (Wang et al. 2020b). 95% (v/v) ethanol was used to remove chlorophyll from the tomato leaves.

Phylogenetic analysis

We performed the multiple sequence alignment and phylogenetic analysis of REC proteins in tomato (*S. lycopersicum*), rice (*O. sativa*), Arabidopsis (*A. thaliana*), monkeyflower (*M. lewisii* and *M. verbenaceus*) using MUSCLE (Edgar 2004). The phylogenetic tree was constructed using MEGA 7.0 software with the maximum likelihood method and 1,000 bootstrap value (Kumar et al. 2016). The posterior probabilities of amino acid sequences were shown as the percentage at branch points.

Exogenous chemical treatments and endogenous ABA content assay

To investigate the role of ABA in *SlREC2*-regulated cold tolerance, 50 μM ABA or 50 μM NDGA (ABA-inhibitor) was applied on leaves of wild-type (pTRV) and *SlREC2*-silenced plants (pTRV-*REC2*) at 12 h prior to exposure to cold conditions at 4 °C for 7 d. We prepared the ABA (Sigma–Aldrich, St. Louis, MO, USA) and NDGA (Sigma–Aldrich, St. Louis, MO, USA) solutions by dissolving the solutes in ethanol followed by dilution with distilled water (ethanol:water [v/v] = 1:10,000), respectively. A 50 mL volume of the solution or water was applied to each plant. ABA content was examined as described previously (Wang et al. 2016, 2020a).

RNA extraction and RT-qPCR analysis

Total RNA was extracted from tomato leaves using an RNAprep Pure Plant Kit (Tiangen Biotech, Beijing, China), and reverse transcribed into cDNA using the ReverTra Ace qPCR RT Kit (Toyobo, Osaka, Japan). The expression levels of target genes were detected by an Applied Biosystems 7,500 Real-Time PCR system (qTower3G, Jena, Germany) with SYBR Green PCR Master Mix Kit (TaKara Bio Inc., Kusatsu, Japan). The tomato *ACTIN2* and *UBI3* genes were used as internal references. Relative gene expression was

calculated as previously described (Livak and Schmittgen 2001). Primer sequences for RT-qPCR are presented in Supplemental Table S2.

Yeast two-hybrid assay

We used the Matchmaker Gold Yeast Two-Hybrid System to build Y2H constructs (Clontech, Mountain View, CA, USA) as previously described (Wang et al. 2022). The full coding sequence (CDS) of SlREC2 and SlBCH1b were cloned into the pGBKT7-BD bait vector and the pGADT7-AD prey plasmid, respectively. The constructs were co-transformed into strain Y2H Gold according to the manufacturer's instructions. The transformants were grown on -Trp/-Leu or -Trp/-Leu/-His/-Ade selective medium for 2 to 3 d. There were 40 μg mL^{-1} of X-α-gal (5-bromo-4-chloro-3-indole-β-D-galactoside) and 100 ng ml^{-1} AbA in the yeast synthetic medium without Trp/Leu/His/Ade for selection as above. PCR primers used for vector construction are listed in Supplemental Table S1.

BiFC assay

The CDS of *SlREC2* without stop codon was cloned into *pSPYNE*, while SlBCH1b was cloned into *pSPYCE*. The fusion plasmids were co-expressed in *N. benthamiana* leaves for 48 h as described previously (Walter et al. 2004). Fluorescence of YFP and 4′,6-diamidino-2-phenylindole (DAPI) was observed and photographed using a confocal laser scanning microscope (TCS SP8; Leica, Wetzlar, Germany). The excitation wavelength of the fluorescent signal is 515 nm (YFP) or 405 nm (DAPI), and the emission wavelength is 525 to 560 nm (YFP) or 420 to 470 nm (DAPI), respectively. Primers used for the vector constructs are listed in Supplemental Table S1.

Subcellular localization analysis

SlREC2 and *SlBCH1b* coding sequences were amplified with specific primers and cloned into the pCAMBIA1300-GFP vector to generate fusion constructs. The fusion constructs were introduced into *Agrobacterium tumefasciens* GV3101 and then infiltrated into *N. benthamiana* leaves. GFP fluorescence signals in infiltrated leaf epidermal cells were captured by a confocal laser scanning microscope (TCS SP8; Leica, Wetzlar, Germany) after 3 d. DAPI fluorescence was used as a nucleus marker. The excitation wavelength of the fluorescent signal is 488 nm (GFP) or 405 nm (DAPI), and the emission wavelength is 500 to 572 nm (GFP) or 420 to 470 nm (DAPI), respectively.

Firefly luciferase complementation imaging assays

The CDS of *SlREC2* was fused with nLUC on the vector pCAMBIA1300-nLUC, while *SlBCH1b* was fused with cLUC on the vector pCAMBIA1300-cLUC (Wang et al. 2022). *Agrobacterium tumefasciens* GV3101 harboring *35S::SlREC2*-nLUC and *35S::*cLUC-*SlBCH1b* were used to co-transform *N. benthamiana* plant leaves. After 3 d, the leaves were treated with 0.2 mmol L^{-1} potassium luciferin (Gold Biotechnology Inc., St Louis, MO, USA) and were used to capture the firefly LUC image with the Night Shade LB 985 system (Berthold, Bad Wildbad, Germany). Primers used for the vector constructs are listed in Supplemental Table S1.

Statistical analysis

The experimental design was a completely randomized design. The significance of differences was determined by ANOVA followed by Tukey's test at $P < 0.05$ using SPSS22 software (IBM Corp., Armonk, NY, USA).

Accession numbers

Sequence data from this article can be obtained from the Sol Genomics databases (https://solgenomics.net/) under the accession numbers listed in Supplemental Table S2.

Supplemental data

The following materials are available in the online version of this article.

Supplemental Figure S1. Identification of REC proteins in tomato.

Supplemental Figure S2. The tomato *SlREC2*-silenced plants.

Supplemental Figure S3. Silencing of *SlREC2* leads to impaired photosynthetic performance index in tomato plants under cold stress.

Supplemental Figure S4. Silencing of *SlREC2* decreases the expression levels of CBF-pathway genes in tomato plants under cold stress.

Supplemental Figure S5. Silencing of *SlREC2* leads to impaired electron transfer rates of photosystem in tomato plants under cold stress.

Supplemental Figure S6. Foliar application of ABA rescues cold tolerance in *SlREC2*-silenced plants.

Supplemental Figure S7. *SlREC2* regulates cold tolerance through the *SlNCED1*-mediated ABA pathway.

Supplemental Figure S8. Subcellular localization of SlBCH1b. The SlBCH1b-GFP fusion protein was expressed in *Nicotiana benthamiana* leaf epidermal cells.

Supplemental Figure S9. The tomato *SlBCH1b*-silenced plants.

Supplemental Figure S10. *SlBCH1b* is important for alleviating cold-induced photoinhibition in tomato.

Supplemental Figure S11. *SlREC2* and *SlBCH1b* act additively to enhance cold tolerance in tomato.

Supplemental Table S1. PCR primer sequences used for vector construction.

Supplemental Table S2. List of primer sequences used for RT-qPCR analysis.

Author contributions

F.W. conceived the project. F.W. and T.L. designed the experiments. Y.Z., F.W., Y.P., J.L., J.Y., K.Z., X.B., X.S., and X.W. performed the research. Y.Z., Y.P., Y.L., X.W., Z.S., M.Q., T.L., and F.W. analyzed and discussed the data. Y.Z., G.A., T.L.,

and F.W. wrote the manuscript with comments from all the authors.

Acknowledgments

We thank Na Cui for the vectors of pCAMBIA1300-nLUC and pCAMBIA1300-cLUC, and the Tomato Genetics Resource Center for tomato seeds.

Funding

This work was supported by grants from the National Natural Science Foundation of China (32122081, 32272698), National Key Research and Development Program of China (2019YFD1000300 and 2018YFD1000800), Liaoning Provincial Natural Science Foundation for Excellent Youth (2022-YQ-18), Young and Middle-aged Science and Technology Innovation Talent Support Program in Shenyang (RC200449), China Agriculture Research System of MOF and MARA (CARS-23), National Natural Science Foundation of China (31801904, 31991184), and Innovative Research Team (Science and Technology) in University of Henan Province (23IRTSTHN024).

Conflict of interest statement. The authors declare no conflict of interest.

References

Agarwal M, Hao Y, Kapoor A, Dong CH, Fujii H, Zheng X, Zhu JK. A R2R3 type MYB transcription factor is involved in the cold regulation of CBF genes and in acquired freezing tolerance. J Biol Chem. 2006:**281**(49):37636–37645. https://doi.org/10.1074/jbc.M605895200

Baker MJ, Frazier AE, Gulbis JM, Ryan MT. Mitochondrial protein-import machinery: correlating structure with function. Trends Cell Biol. 2007:**17**(9):456–464. https://doi.org/10.1016/j.tcb.2007.07.010

Baroli I, Niyogi KK. Molecular genetics of xanthophyll-dependent photoprotection in green algae and plants. Philos Trans R Soc Lond B Biol Sci. 2000:**355**(1402):1385–1393. https://doi.org/10.1098/rstb.2000.0700

Boudreau E, Nickelsen J, Lemaire SD, Ossenbuhl F, Rochaix JD. The Nac2 gene of chlamydomonas encodes a chloroplast TPR-like protein involved in psbD mRNA stability. EMBO J. 2000:**19**(13):3366–3376. https://doi.org/10.1093/emboj/19.13.3366

Bouvier F, Keller Y, d'Harlingue A, Camara B. Xanthophyll biosynthesis: molecular and functional characterization of carotenoid hydroxy-lases from pepper fruits (*Capsicum annuum* L.). Biochim Biophys Acta. 1998:**1391**(3):320–328. https://doi.org/10.1016/S0005-2760(98)00029-0

Brocard C, Hartig A. Peroxisome targeting signal 1: is it really a simple tripeptide? Biochim Biophys Acta. 2006:**1763**(12):1565–1573. https://doi.org/10.1016/j.bbamcr.2006.08.022

Bu X, Wang XJ, Yan JR, Zhang Y, Zhou SY, Sun X, Yang YX, Ahammed GJ, Liu YF, Qi MF, et al. Genome-wide characterization of *B-box* gene family and its roles in responses to light quality and cold stress in tomato. Front Plant Sci. 2021:**12**:698525. https://doi.org/10.3389/fpls.2021.698525

Cerveny L, Straskova A, Dankova V, Hartlova A, Ceckova M, Staud F, Stulik J. Tetratricopeptide repeat motifs in the world of bacterial pathogens: role in virulence mechanisms. Infect Immun. 2013:**81**(3):629–635. https://doi.org/10.1128/IAI.01035-12

Chen X, Ding Y, Yang Y, Song C, Wang B, Yang S, Guo Y, Gong Z. Protein kinases in plant responses to drought, salt, and cold stress. J Integr Plant Biol. 2021:**63**(1):53–78. https://doi.org/10.1111/jipb.13061

Chinnusamy V, Ohta M, Kanrar S, Lee BH, Hong X, Agarwal M, Zhu JK. ICE1: a regulator of cold-induced transcriptome and freezing tolerance in *Arabidopsis*. Genes Dev. 2003:**17**(8):1043–1054. https://doi.org/10.1101/gad.1077503

D'Ambrosio C, Stigliani AL, Giorio G. Overexpression of *CrtR-b2* (carotene beta hydroxylase 2) from *S. lycopersicum* L. Differentially affects xanthophyll synthesis and accumulation in transgenic tomato plants. Transgenic Res. 2011:**20**(1):47–60. https://doi.org/10.1007/s11248-010-9387-4

Dall'Osto L, Fiore A, Cazzaniga S, Giuliano G, Bassi R. Different roles of alpha- and beta-branch xanthophylls in photosystem assembly and photoprotection. J Biol Chem. 2007:**282**(48):35056–35068. https://doi.org/10.1074/jbc.M704729200

Ding Y, Jia Y, Shi Y, Zhang X, Song C, Gong Z, Yang S. OST1-mediated BTF3L phosphorylation positively regulates *CBFs* during plant cold responses. EMBO J. 2018:**37**(8):e98228. https://doi.org/10.15252/embj.201798228

Ding Y, Li H, Zhang X, Xie Q, Gong Z, Yang S. OST1 kinase modulates freezing tolerance by enhancing ICE1 stability in *Arabidopsis*. Dev Cell. 2015:**32**(3):278–289. https://doi.org/10.1016/j.devcel.2014.12.023

Ding Y, Shi Y, Yang S. Molecular regulation of plant responses to environmental temperatures. Mol Plant. 2020:**13**(4):544–564. https://doi.org/10.1016/j.molp.2020.02.004

Edgar RC. MUSCLE: multiple sequence alignment with high accuracy and high throughput. Nucleic Acids Res. 2004:**32**(5):1792–1797. https://doi.org/10.1093/nar/gkh340

Gong Z, Xiong L, Shi H, Yang S, Herrera-Estrella LR, Xu G, Chao DY, Li J, Wang PY, Qin F, et al. Plant abiotic stress response and nutrient use efficiency. Sci China Life Sci. 2020:**63**(5):635–674. https://doi.org/10.1007/s11427-020-1683-x

Guo X, Liu D, Chong K. Cold signaling in plants: insights into mechanisms and regulation. J Integr Plant Biol. 2018:**60**(9):745–756. https://doi.org/10.1111/jipb.12706

Heinnickel M, Kim RG, Wittkopp TM, Yang W, Walters KA, Herbert SK, Grossman AR. Tetratricopeptide repeat protein protects photosystem I from oxidative disruption during assembly. Proc Natl Acad Sci U S A. 2016:**113**(10):2774–2779. https://doi.org/10.1073/pnas.1524040113

Hu Z, Xu F, Guan L, Qian P, Liu Y, Zhang H, Huang Y, Hou S. The tetratricopeptide repeat-containing protein slow green1 is required for chloroplast development in *Arabidopsis*. J Exp Bot. 2014:**65**(4):1111–1123. https://doi.org/10.1093/jxb/ert463

Jahns P, Latowski D, Strzalka K. Mechanism and regulation of the violaxanthin cycle: the role of antenna proteins and membrane lipids. Biochim Biophys Acta. 2009:**1787**(1):3–14. https://doi.org/10.1016/j.bbabio.2008.09.013

Kalaji HM, Oukarroum A, Alexandrov V, Kouzmanova M, Brestic M, Zivcak M, Samborska IA, Cetner MD, Allakhverdiev SI, Goltsev V. Identification of nutrient deficiency in maize and tomato plants by in vivo chlorophyll a fluorescence measurements. Plant Physiol Biochem. 2014:**81**:16–25. https://doi.org/10.1016/j.plaphy.2014.03.029

Kalanon M, McFadden GI. The chloroplast protein translocation complexes of *Chlamydomonas reinhardtii*: a bioinformatic comparison of Toc and Tic components in plants, green algae and red algae. Genetics. 2008:**179**(1):95–112. https://doi.org/10.1534/genetics.107.085704

Kim J, Smith J, Tian L, DellaPenna D. The evolution and function of carotenoid hydroxylases in *Arabidopsis*. Plant Cell Physiol. 2009:**50**(3):463–479. https://doi.org/10.1093/pcp/pcp005

Kingston-Smith AH, Harbinson J, Williams J, Foyer CH. Effect of chilling on carbon assimilation, enzyme activation, and photosynthetic electron transport in the absence of photoinhibition in maize leaves. Plant Physiol. 1997:**114**(3):1039–1046. https://doi.org/10.1104/pp.114.3.1039

Kromdijk J, Głowacka K, Leonelli L, Gabilly ST, Iwai M, Niyogi KK, Long SP. Improving photosynthesis and crop productivity by accelerating recovery from photoprotection. Science. 2016:**354**(6314):857–861. https://doi.org/10.1126/science.aai8878

Kumar S, Stecher G, Tamura K. MEGA7: molecular evolutionary genetics analysis version 7.0 for bigger datasets. Mol Biol Evol. 2016:**33**(7):1870–1874. https://doi.org/10.1093/molbev/msw054

Lamb JR, Tugendreich S, Hieter P. Tetratrico peptide repeat interactions: to TPR or not to TPR? Trends Biochem Sci. 1995:**20**(7):257–259. https://doi.org/10.1016/S0968-0004(00)89037-4

Lang Z, Zhu J. OST1 phosphorylates ICE1 to enhance plant cold tolerance. Sci China Life Sci. 2015:**58**(3):317–318. https://doi.org/10.1007/s11427-015-4822-7

Larkin RM, Stefano G, Ruckle ME, Stavoe AK, Sinkler CA, Brandizzi F, Malmstrom CM, Osteryoung KW. *REDUCED CHLOROPLAST COVERAGE* genes from *Arabidopsis thaliana* help to establish the size of the chloroplast compartment. Proc Natl Acad Sci USA. 2016:**113**(8):E1116–E1125. https://doi.org/10.1073/pnas.1515741113

Lesk C, Rowhani P, Ramankutty N. Influence of extreme weather disasters on global crop production. Nature. 2016:**529**(7584):84–87. https://doi.org/10.1038/nature16467

Lin Z, Arciga-Reyes L, Zhong S, Alexander L, Hackett R, Wilson I, Grierson D. SlTPR1, a tomato tetratricopeptide repeat protein, interacts with the ethylene receptors NR and LeETR1, modulating ethylene and auxin responses and development. J Exp Bot. 2008:**59**(15):4271–4287. https://doi.org/10.1093/jxb/ern276

Lin Z, Ho CW, Grierson D. AtTRP1 encodes a novel TPR protein that interacts with the ethylene receptor ERS1 and modulates development in Arabidopsis. J Exp Bot. 2009:**60**(13):3697–3714. https://doi.org/10.1093/jxb/erp209

Liu CT, Ou SJ, Mao BG, Tang JY, Wang W, Wang H, Cao SY, Schlappi MR, Zhao BG, Xiao GY, et al. Early selection of bZIP73 facilitated adaptation of japonica rice to cold climates. Nat Commun. 2018a:**9**(1):3302. https://doi.org/10.1038/s41467-018-05753-w

Liu CT, Wang W, Mao BG, Chu CC. Cold stress tolerance in rice: physiological changes, molecular mechanism, and future prospects. Hereditas. 2018b:**40**(3):171–185. https://doi.org/10.16288/j.yczz.18-007

Livak KJ, Schmittgen TD. Analysis of relative gene expression data using real-time quantitative PCR and the 2[-Delta DeltaC(T)] method. Methods. 2001:**25**(4):402–408. https://doi.org/10.1006/meth.2001.1262

Marin E, Nussaume L, Quesada A, Gonneau M, Sotta B, Hugueney P, Frey A, Marion-Poll A. Molecular identification of zeaxan-thin epoxidase of *Nicotiana plumbaginifolia*, a gene involved in abscisic acid biosynthesis and corresponding to the ABA locus of *Arabidopsis thaliana*. EMBO J. 1996:**15**(10):2331–2342. https://doi.org/10.1002/j.1460-2075.1996.tb00589.x

Merchante C, Alonso JM, Stepanova AN. Ethylene signaling: simple ligand, complex regulation. Curr Opin Plant Biol. 2013:**16**(5):554–560. https://doi.org/10.1016/j.pbi.2013.08.001

Mirus O, Bionda T, von Haeseler A, Schleiff E. Evolutionarily evolved discriminators in the 3-TPR domain of the Toc64 family involved in protein translocation at the outer membrane of chloroplasts and mitochondria. J Mol Model. 2009:**15**(8):971–982. https://doi.org/10.1007/s00894-008-0449-y

Muller P, Li XP, Niyogi KK. Non-photochemical quenching. A response to excess light energy. Plant Physiol. 2001:**125**(4):1558–1566. https://doi.org/10.1104/pp.125.4.1558

Murata N, Los DA. Histidine kinase Hik33 is an important participant in cold-signal transduction in cyanobacteria. Physiol Plant. 2006:**126**(1):17–27. https://doi.org/10.1111/j.1399-3054.2006.00608.x

Naver H, Boudreau E, Rochaix JD. Functional studies of Ycf3: its role in assembly of photosystem I and interactions with some of its subunits. Plant Cell. 2001:**13**(12):2731–2745. https://doi.org/10.1105/tpc.010253

Niyogi KK, Grossman AR, Björkman O. Arabidopsis mutants define a central role for the xanthophyll cycle in the regulation of photosynthetic energy conversion. Plant Cell. 1998:**10**(7):1121–1134. https://doi.org/10.1105/tpc.10.7.1121

Park MY, Kang JY, Kim SY. Overexpression of *AtMYB52* confers ABA hypersensitivity and drought tolerance. Mol Cells. 2011:**31**(5):447–454. https://doi.org/10.1007/s10059-011-0300-7

Park S, Khamai P, Garcia-Cerdan JG, Melis A. REP27, a tetratricopeptide repeat nuclear-encoded and chloroplast-localized protein, functions in D1/32-kD reaction center protein turnover and photosystem II repair from photodamage. Plant Physiol. 2007:**143**(4):1547–1560. https://doi.org/10.1104/pp.107.096396

Peng L, Ma J, Chi W, Guo J, Zhu S, Lu Q, Lu C, Zhang L. LOW PSII ACCUMULATION1 is involved in efficient assembly of photosystem II in *Arabidopsis thaliana*. Plant Cell. 2006:**18**(4):955–969. https://doi.org/10.1105/tpc.105.037689

Pfalz J, Liere K, Kandlbinder A, Dietz KJ, Oelmuller R. pTAC2, -6, and -12 are components of the transcriptionally active plastid chromosome that are required for plastid gene expression. Plant Cell. 2006:**18**(1):176–197. https://doi.org/10.1105/tpc.105.036392

Rosado A, Schapire AL, Bressan RA, Harfouche AL, Hasegawa PM, Valpuesta V, Botella MA. The Arabidopsis tetratricopeptide repeat-containing protein TTL1 is required for osmotic stress responses and abscisic acid sensitivity. Plant Physiol. 2006:**142**(3):1113–1126. https://doi.org/10.1104/pp.106.085191

Sagawa JM, Stanley LE, LaFountain AM, Frank HA, Liu C, Yuan YW. An R2R3-MYB transcription factor regulates carotenoid pigmentation in *Mimulus lewisii* flowers. New Phytol. 2016:**209**(3):1049–1057. https://doi.org/10.1111/nph.13647

Schottkowski M, Ratke J, Oster U, Nowaczyk M, Nickelsen J. Pitt, a novel tetratricopeptide repeat protein involved in light dependent chlorophyll biosynthesis and thylakoid membrane biogenesis in *Synechocystis sp.* PCC 6803. Mol Plant. 2009:**2**(6):1289–1297. https://doi.org/10.1093/mp/ssp075

Shi Y, Ding Y, Yang S. Molecular regulation of CBF signaling in cold acclimation. Trends Plant Sci. 2018:**23**(7):623–637. https://doi.org/10.1016/j.tplants.2018.04.002

Shi Y, Tian S, Hou L, Huang X, Zhang X, Guo H, Yang S. Ethylene signaling negatively regulates freezing tolerance by repressing expression of CBF and type-A ARR genes in Arabidopsis. Plant Cell. 2012:**24**(6):2578–2595. https://doi.org/10.1105/tpc.112.098640

Shimura Y, Shiraiwa Y, Suzuki I. Characterization of the subdomains in the N-terminal region of histidine kinase Hik33 in the cyanobacterium Synechocystis sp. PCC 6803. Plant Cell Physiol. 2012:**53**:1255–1266

Sohrt K, Soll J. Toc64, a new component of the protein translocon of chloroplasts. J Cell Biol. 2000:**148**(6):1213–1222. https://doi.org/10.1083/jcb.148.6.1213

Song Y, Zhang X, Li M, Yang H, Fu D, Lv J, Ding Y, Gong Z, Shi Y, Yang S. The direct targets of CBFs: in cold stress response and beyond. J Integr Plant Biol. 2021:**63**(11):1874–1887. https://doi.org/10.1111/jipb.13161

Stanley LE, Ding B, Sun W, Mou F, Hill C, Chen S, Yuan YW. A tetratricopeptide repeat protein regulates carotenoid biosynthesis and chromoplast development in monkeyflowers (*Mimulus*). Plant Cell. 2020:**32**(5):1536–1555. https://doi.org/10.1105/tpc.19.00755

Stockel J, Bennewitz S, Hein P, Oelmuller R. The evolutionarily conserved tetratrico peptide repeat protein pale yellow green7 is required for photosystem I accumulation in *Arabidopsis* and copurifies with the complex. Plant Physiol. 2006:**141**(3):870–878. https://doi.org/10.1104/pp.106.078147

Stockinger EJ, Gilmour SJ, Thomashow MF. *Arabidopsis thaliana* CBF1 encodes an AP2 domain-containing transcriptional activator

that binds to the C-repeat/DRE, a cis-acting DNA regulatory element that stimulates transcription in response to low temperature and water deficit. Proc Natl Acad Sci USA. 1997:**94**(3):1035–1040. https://doi.org/10.1073/pnas.94.3.1035

Sundby C, McCaffery S, Anderson JM. Turnover of the photosystem II D1 protein in higher plants under photoinhibitory and nonphotoinhibitory irradiance. J Biol Chem. 1993:**268**(34):25476–25482. https://doi.org/10.1016/S0021-9258(19)74416-0

Takahashi S, Badger MR. Photoprotection in plants: a new light on photosystem II damage. Trends Plant Sci. 2011:**16**(1):53–60. https://doi.org/10.1016/j.tplants.2010.10.001

Thomashow MF. Plant cold acclimation: freezing tolerance genes and regulatory mechanisms. Annu Rev Plant Physiol Plant Mol Biol. 1999:**50**(1):571–599. https://doi.org/10.1146/annurev.arplant.50.1.571

Vaistij FE, Goldschmidt-Clermont M, Wostrikoff K, Rochaix JD. Stability determinants in the chloroplast psbB/T/H mRNAs of Chlamydomonas reinhardtii. Plant J. 2000:**21**(5):469–482. https://doi.org/10.1046/j.1365-313x.2000.00700.x

Walter M, Chaban C, Schutze K, Batistic O, Weckermann K, Nake C, Blazevic D, Grefen C, Schumacher K, Oecking C, et al. Visualization of protein interactions in living plant cells using bimolecular fluorescence complementation. Plant J. 2004:**40**(3):428–438. https://doi.org/10.1111/j.1365-313X.2004.02219.x

Walter MH, Strack D. Carotenoids and their cleavage products: biosynthesis and functions. Nat Prod Rep. 2011:**28**(4):663–692. https://doi.org/10.1039/c0np00036a

Wang F, Chen XX, Dong SJ, Jiang XC, Wang LY, Yu JQ, Zhou YH. Crosstalk of PIF4 and DELLA modulates CBF transcript and hormone homeostasis in cold response in tomato. Plant Biotechnol J. 2020a:**18**(4):1041–1055. https://doi.org/10.1111/pbi.13272

Wang F, Guo ZX, Li HZ, Wang MM, Onac E, Zhou J, Xia XJ, Shi K, Yu JQ, Zhou YH. Phytochrome A and B function antagonistically to regulate cold tolerance via abscisic acid-dependent jasmonate signaling. Plant Physiol. 2016:**170**(1):459–471. https://doi.org/10.1104/pp.15.01171

Wang F, Wang XJ, Zhang Y, Yan JR, Ahammed GJ, Bu X, Sun X, Liu YF, Xu T, Qi HY, et al. SlFHY3 and SlHY5 act compliantly to enhance cold tolerance through the integration of myo-inositol and light signaling in tomato. New Phytol. 2022:**233**(5):2127–2143. https://doi.org/10.1111/nph.17934

Wang F, Wu N, Zhang LY, Ahammed GJ, Chen XX, Xiang X, Zhou J, Xia XJ, Shi K, Yu JQ, et al. Light signaling-dependent regulation of photoinhibition and photoprotection in tomato. Plant Physiol. 2018:**176**(2):1311–1326. https://doi.org/10.1104/pp.17.01143

Wang F, Yan JR, Ahammed GJ, Wang XJ, Bu X, Xiang HZ, Li YB, Lu JZ, Liu YF, Qi HY, et al. PGR5/PGRL1 and NDH mediate far-red light-induced photoprotection in response to chilling stress in tomato. Front Plant Sci. 2020b:**11**:669. https://doi.org/10.3389/fpls.2020.00669

Wang F, Zhang LY, Chen XX, Wu XD, Xiang X, Zhou J, Xia XJ, Shi K, Yu JQ, Foyer CH, et al. *SlHY5* integrates temperature, light and hormone signaling to balance plant growth and cold tolerance. Plant Physiol. 2019a:**179**(2):749–760. https://doi.org/10.1104/pp.18.01140

Wang X, Ding YL, Li ZY, Shi YT, Wang JL, Hua J, Gong ZZ, Zhou JM, Yang SH. PUB25 and PUB26 promote plant freezing tolerance by degrading the cold signaling negative regulator MYB15. Dev Cell. 2019b:**51**(2):222–235. https://doi.org/10.1016/j.devcel.2019.08.008

Whitfield C, Mainprize IL. TPR motifs: hallmarks of a new polysaccharide export scaffold. Structure. 2010:**18**(2):151–153. https://doi.org/10.1016/j.str.2010.01.006

Young JC, Barral JM, Ulrich Hartl F. More than folding: localized functions of cytosolic chaperones. Trends Biochem Sci. 2003:**28**(10):541–547. https://doi.org/10.1016/j.tibs.2003.08.009

Zhang L, Zhang F, Zhou X, Poh TX, Xie L, Shen J, Yang L, Song S, Yu H, Chen Y. The tetratricopeptide repeat protein OsTPR075 promotes heading by regulating florigen transport in rice. Plant Cell. 2022:**34**(10):3632–3646. https://doi.org/10.1093/plcell/koac190

Zhao C, Zhang Z, Xie S, Si T, Li Y, Zhu JK. Mutational evidence for the critical role of CBF transcription factors in cold acclimation in *Arabidopsis*. Plant Physiol. 2016:**171**(4):2744–2759. https://doi.org/10.1104/pp.16.00533